UNITU-THEP-16/1994
August 1994
hep-ph/9408343

Estimate of Quantum corrections to the Mass of the Chiral Soliton in the Nambu–Jona–Lasinio Model

H. Weigel†, R. Alkofer, and H. Reinhardt

Institute for Theoretical Physics
Tübingen University
Auf der Morgenstelle 14
D-72076 Tübingen, Germany

ABSTRACT

The Bethe–Salpeter equation for pion fluctuations off the chiral soliton in the Nambu–Jona–Lasinio model is constructed. By Goldstone's theorem this equation has rotational and translational zero modes because the classical soliton is a localized stationary field configuration which violates rotational and translational invariance. Furthermore, the proper normalization of the fluctuating eigen–modes is obtained. Second quantization of the pion fluctuations off the chiral soliton provides an energy functional of the pion fluctuations which formally coincides with that of a harmonic oscillator. The corresponding quantum corrections to the soliton mass together with the semi–classical cranking prescription yield reasonable predictions for the masses of the nucleon and the Δ–resonance when the constituent quark mass is chosen to be about 400MeV. These calculations are, to some extend, hampered by the non–confining character of the Nambu–Jona–Lasinio model. Comments on the $1/N_C$ counting scheme are added.

† Supported by a Habilitanden–scholarship of the Deutsche Forschungsgemeinschaft (DFG).

1. Introduction

In recent years it has turned out that soliton solutions of mesonic theories provide quite a reasonable description of baryons. These approaches are motivated by generalizing Quantum Chromo Dynamics (QCD), which is widely believed to represent the theory of strong interaction, to an arbitrary number of color degrees of freedom (N_C) [1]. In the limit $N_C \to \infty$, QCD reduces to an effective theory of weakly interating mesons (and glueballs); the effective coupling constant being of the order $1/N_C$ [1, 2]. From the fact that baryon masses increase linear in N_C, *i.e.* reciprocal to the effective coupling constant, Witten conjectured [2] that baryons emerge as soliton solutions of the effective theory. It is a common feature of solitons that their energies increase with the inverse coupling constant. These ideas have been brought to practice in the work of Adkins, Nappi and Witten [3] by reviving the Skyrme model [4] from the early sixties. The original Skyrme model consists of the non–linear σ–model and an antisymmetric forth order (in derivatives) term which is mandatory to obtain stable soliton solutions. This model has in turn been applied to investigate many properties of baryons [5]. Examples are electromagnetic form factors [6] or the phase shift analysis of pion–nucleon scattering [7, 8]. Over the past decade the Skyrme model then has experienced quite an amount of extensions*. *E.g.* vector mesons have been added [10] and the three flavor version of the model has been investigated in detail†. All these extensions were performed such as to comply with the basic symmetries of QCD, in particular the chiral symmetry. It has turned out that all these models provide a reasonable, not to say successful, description of baryon properties. As a prominent example one may quote the natural description of the smallness of the matrix element of the axial singlet current, *i.e.* the famous proton spin puzzle [11]. Unfortunately, one big problem has remained unsolved over the years: The too large prediction for the absolute mass of the nucleon. Adopting parameters which are fixed in the meson sector as far as possible the nucleon mass is overestimated by about 50%, in three flavor models even more. It has only been very recently that quantum corrections to the mass of the Skyrmion have been evaluated [12, 13, 14]. Indeed these have been found to provide a sizable reduction of the soliton mass leading to a predicted nucleon mass just of the right magnitude.

As a matter of fact these corrections, which are due to mesonic loops, can be classified by the $1/N_C$–expansion. As the absolute mass of the nucleon (938MeV) is in leading order proportional to N_C, the quantum corrections are of one order less, N_C^0. Empirically the size of these corrections can be estimated from the mass difference between the nucleon and the Roper resonance (1440MeV) to be about 500MeV. The third order in this expansion (N_C^{-1}) may be read off from the difference between the nucleon mass and the position of the Δ–resonance (1232MeV). The numerical results in the Skyrme model have been seen to follow this pattern. The mass of the Skyrmion is found to be about 1.7–2.0GeV while quantum corrections are somewhat less than 1GeV [14]. The mass difference between the nucleon and the Δ–resonance is commonly employed to adjust the only free parameter in the baryon sector of the Skyrme model. One may summarize these studies in the Skyrme model by stating that the problem of the too large nucleon mass in these models has, to a large extend, been solved. What remains to be considered are the analogue quantum corrections to other observables.

The investigations in the Skyrme model have revealed one important fact for the evaluation of such quantum corrections [14]: the dominant contribution (about 90%) is due to

*For a compilation of citations see ref. [9].

†*Cf.* chapter III of ref. [9].

the zero–modes of the soliton while the contribution of the continuum (or scattering) states is almost negligible. These zero–modes arise because the soliton configuration breaks the spin (isospin) and translational symmetries of the model. As the quantum corrections are naturally subject to subtracting the counterpart associated with the trivial vacuum, which does not contain these zero modes but rather possesses a mass gap, it is obvious that the zero modes may provide a sizable contribution. The details of this issue will become more quantitative in the course of this paper.

Only a little after the rediscovery of the Skyrme model it has been shown that the bosonized version[15] of the Nambu and Jona–Lasinio (NJL) model [16, 17] also contains soliton solutions [18]. Although the NJL model is not as feasible as the Skyrme model the NJL model is in a sense superior because it represents a microscopic theory of the quark flavor dynamics. The major purpose of the present paper is to examine the corrections to the mass of the NJL soliton stemming from quantum fluctuations. In many parts this will be similar to the analogous Skyrme model calculations [14], however, in the NJL model new features will arise since the meson fields here are composite fields built up from quarks rather than being elementary as it is the case in the Skyrme model. For example the dependence of the action on the derivative of the meson fields with respect to the time coordinate, which is essential for the canonical quantization, is not explicitly known. As already mentioned it is necessary to subtract the energy of the trivial vacuum (the baryon number zero configuration). In the NJL model this provides a further complication because in the baryon number zero sector the meson fields do not represent solutions of the Klein–Gordon equation as in the Skyrme model but rather of a more involved Bethe–Salpeter equation reflecting the quark substructure of mesons. A further motivation for the evaluation of the quantum corrections to the mass of the NJL soliton is the fact that its classical mass is several hundred MeV lower than the mass of the Skyrmion. It is thus interesting to see whether a similar reduction occurs for the corrections and whether this will in turn lead to a good prediction for the nucleon mass in the NJL model as well.

In order to address these questions we have organized the paper as follows. In the remainder of this introductory section we describe the NJL model and the appearance of its soliton solutions. In section 2 we will introduce small amplitude fluctuations off this soliton and briefly review the derivation of the Bethe–Salpeter equation for meson fluctuations off the soliton. A thorough study of this equation will provide a suitable normalization of the fluctuating modes. In contrast to Skyrme type models this analysis will also be relevant for fluctuations in the baryon number zero sector. In section 3 this normalization will then prove to be useful in order to derive an energy functional for the meson fluctuations. It will be found that these may indeed be quantized using the formalism of second quantization. This in turn allows us to apply techniques which have previously been developed in the context of the Skyrme model [14]. Section 4 is devoted to the discussion of the meson fluctuations in the NJL model in channels which contain zero modes. In section 5 we will numerically evaluate the contribution of the zero modes to the quantum correction of the soliton mass and furthermore make plausible that the contributions of the scattering modes are negligible. Concluding remarks are left to section 6.

As the NJL model is originally formulated in terms of quark degrees of freedom [16] it may be understood as a microscopic model for the quark flavor dynamics. As a matter of fact it can be motivated in the large N_C limit of QCD when the gluon propagator is assumed to behave like a δ–function in coordinate space [19]. More importantly the NJL model exhibits the chiral symmetry and its spontaneous breaking [16]. The latter is reflected by a non–zero vacuum expectation value of the quark condensate $\langle \bar{q}q \rangle$. In the

process of bosonization one introduces composite meson fields which allow one to integrate out the quark degrees of freedom [15]. The resulting action, $\mathcal{A}_{\rm NJL}$, can then be expressed as the sum of a purely mesonic part

$$\mathcal{A}_m = \int d^4x \left(-\frac{1}{4G_{\rm NJL}} {\rm tr}(M^\dagger M - \hat{m}^0(M + M^\dagger) + (\hat{m}^0)^2) \right) \tag{1.1}$$

and a fermion determinant

$$\mathcal{A}_F = {\rm Tr}\log(i\not{D}) = {\rm Tr}\log\left(i\partial\!\!\!/ - (P_R M + P_L M^\dagger) \right), \tag{1.2}$$

i.e.

$$\mathcal{A}_{NJL} = \mathcal{A}_F + \mathcal{A}_m. \tag{1.3}$$

Here $P_{R,L} = (1 \pm \gamma_5)/2$ denote the projectors onto right– and left–handed quark fields, respectively. As indicated in the above expressions (1.1,1.2) we will constrains ourselves to the investigation of scalar (S) and pseudoscalar (P) fields only. These are parametrized by $M = S + iP$ with $S_{ij} = S^a \tau^a_{ij}/2$ and $P_{ij} = P^a \tau^a_{ij}/2$ representing matrix fields in the two dimensional flavor space. Alternatively one may define a polar decomposition of the meson fields

$$M = \xi_L^\dagger \Sigma \xi_R. \tag{1.4}$$

Here the matrix Σ is Hermitian whereas the matrices $\xi_{L,R}$ are unitary. This also gives a natural definition of the chiral field $U = \xi_L^\dagger \xi_R$. In eqn (1.1) $G_{\rm NJL}$ and $\hat{m}^0 = {\rm diag}\,(m_u^0, m_d^0)$ denote the dimensionful NJL coupling constant and the current quark mass matrix. For simplicity we will assume isospin symmetry, *i.e.* $m_u^0 = m_d^0 =: m^0$.

As it stands the action is not well–defined because the fermion determinant diverges and hence needs regularization. This is accomplished by first continuing to Euclidean space $x_0 \to i\tau$ and then considering real and imaginary parts

$$\mathcal{A}_R = \frac{1}{2}{\rm Tr}\,\log\left(\not{D}_E \not{D}_E{}^\dagger \right), \qquad \mathcal{A}_I = \frac{1}{2}{\rm Tr}\,\log\left(\not{D}_E (\not{D}_E{}^\dagger)^{-1} \right). \tag{1.5}$$

of the Euclidean fermion determinant separately. Here it is important to remark that the Euclidean time, τ, has to be considered as a real quantity. Furthermore $\not{D}_E$ is the Euclidean Dirac operator which is obtained from $\not{D}$ by the analytic continuation described above. As a matter of fact only $\mathcal{A}_R$ is divergent and will be regularized by employing Schwinger's proper–time description [20]. This introduces a new parameter, the cut–off Λ, via

$$\mathcal{A}_R \longrightarrow -\frac{1}{2}{\rm Tr}\int_{1/\Lambda^2}^\infty \frac{ds}{s}\,\exp\left(-s \not{D}_E \not{D}_E{}^\dagger \right). \tag{1.6}$$

For a sufficiently large coupling $G_{\rm NJL}$ the scalar field possesses a non–zero vacuum expectation value $\langle\Sigma\rangle = {\rm diag}(m, m)$ which is related to the current quark mass m^0 and the quark condensate $\langle\bar{q}q\rangle$ via the gap equation [15]

$$m \;=\; m^0 + m^3 \frac{N_C G_{\rm NJL}}{2\pi^2} \Gamma\left(-1, (\frac{m}{\Lambda})^2 \right) = m^0 - 2G_{\rm NJL}\langle\bar{q}q\rangle. \tag{1.7}$$

The quantity m is commonly referred to as the constituent quark mass. Actually the non–trivial solutions to eqn (1.7) reflect the spontaneous breaking of the chiral symmetry by a non–vanishing quark condensate $\langle\bar{q}q\rangle$. In order to determine the parameters $G_{\rm NJL}, \Lambda$ and m the fermion determinant is expanded in terms of the meson fields and their derivatives. This then yields an effective meson theory which allows one to express physical quantities like the pion decay constant f_π in terms of the cut–off Λ and the constituent quark mass m [15]

$$f_\pi^2 = \frac{N_C m^2}{4\pi^2}\Gamma\left(0, \left(\frac{m}{\Lambda}\right)^2\right). \tag{1.8}$$

In practice the physical value $f_\pi = 93$MeV is substituted in order to determine Λ for a given constituent quark mass m. Finally $G_{\rm NJL}$ is determined via $G_{\rm NJL} = m^0 m/m_\pi^2 f_\pi^2$ where $m_\pi = 135$MeV denotes the pion mass. Then m is left as the only undetermined quantity.

In order to examine static soliton configurations it is useful to introduce the Dirac Hamiltonian h via

$$i\beta\not{D}_E = -\partial_\tau - h. \tag{1.9}$$

It should be noted that for static configurations only the real part of the fermion determinant is non–zero. The functional trace in eqn (1.6) is performed in two consecutive steps. First one introduces eigenstates[‡] $\Omega_n = (2n+1)\pi/T$ of ∂_τ. Here T denotes the Euclidean time interval under consideration. The fermion determinant has been shown [21] to acquire contributions from the occupation of the valence quark orbit $-TE_{\rm val}[M]$ and the polarized Dirac sea $-TE_{\rm vac}[M]$. Whence the total energy due to the fermion determinant is given by the sum $E_{\rm val}[M] + E_{\rm vac}[M] - E_{\rm vac}[M = m]$, which is a functional of the meson fields M. Also the subtraction due to the trivial configuration is indicated. Defining eigenstates of the Dirac Hamiltonian

$$h\Psi_\nu = \epsilon_\nu \Psi_\nu \tag{1.10}$$

the valence quark part, $E_{\rm val}[M]$, may be expressed as [21]

$$E_{\rm val}[M] = N_C \sum_\nu \eta_\nu |\epsilon_\nu| \tag{1.11}$$

wherein $\eta_\nu = 0, 1$ denote the valence quark occupation number which have to be adjusted such that the total baryon number

$$B = \sum_\nu \left(\eta_\nu - \frac{1}{2}\right) {\rm sgn}(\epsilon_\nu). \tag{1.12}$$

equals unity. The contribution to the energy due to the polarized Dirac sea is obtained from $\mathcal{A}_R$ in the limit $T \to \infty$. Then the temporal part of the functional trace reduces to a spectral integral while the remainder of this trace is performed by summing over the eigenstates of h. These manipulations result in [21]

$$E_{\rm vac}[M] = \frac{N_C}{2}\int_{1/\Lambda^2}^\infty \frac{ds}{\sqrt{4\pi s^3}} \sum_\nu \exp\left(-s\epsilon_\nu^2\right). \tag{1.13}$$

[‡]Ω_n are the Matsubara frequencies. The fermionic character of the quarks requires anti–periodic boundary conditions.

The classical soliton energy is finally given by the sum

$$E_{\rm cl}[M] = E_{\rm val}[M] + E_{\rm vac}[M] - E_{\rm vac}[M=m] + E_m[M] \tag{1.14}$$

wherein $E_m[M]$ originates from the mesonic part of the action (1.1).

To be specific we employ the hedgehog *ansatz* for the chiral field (in unitary gauge $\xi_L^\dagger = \xi_R = \xi$)[§]

$$\xi_0(\boldsymbol{r}) = \exp\left(\frac{i}{2}\boldsymbol{\tau}\cdot\hat{\boldsymbol{r}}\;\Theta(r)\right) \tag{1.15}$$

while the scalar fields are constrained to the chiral circle, $\Sigma = \langle\Sigma\rangle = m$. Substituting this *ansatz* into the Dirac Hamiltonian (1.9) yields

$$h_0 = \boldsymbol{\alpha}\cdot\boldsymbol{p} + \beta m\left(\cos\Theta(r) + i\gamma_5\boldsymbol{\tau}\cdot\hat{\boldsymbol{r}}\;\sin\Theta(r)\right). \tag{1.16}$$

This Hamiltonian possesses the celebrated feature to commute with both parity ($\hat{\Pi}$) and grand spin operators ($\boldsymbol{G} = \boldsymbol{l} + \boldsymbol{\sigma}/2 + \boldsymbol{\tau}/2$). The latter is the sum of orbital angular momentum ($\boldsymbol{l}$), spin ($\boldsymbol{\sigma}/2$) and isopin ($\boldsymbol{\tau}/2$) operators. Thus the eigenstates Ψ_ν fall into independent subspaces which are characterized by the eigenvalues of $\hat{\Pi}$ and $\boldsymbol{G}$. For the hedgehog *ansatz* the mesonic part of the energy is given by

$$E_m[\Theta] = 4\pi m_\pi^2 f_\pi^2 \int dr r^2\left(1-\cos\Theta(r)\right). \tag{1.17}$$

The stationary condition $\delta E_{\rm cl}[\Theta]/\delta\Theta = 0$ is obtained using the chain rule. First the energy functional is differentiated with respect to the one–particle energies ϵ_ν. Subsequently these eigenvalues are functionally differentiated with respect to $\Theta(r)$. This leads to the equation of motion

$$\cos\Theta(r)\;{\rm tr}\int d\Omega\;\rho^S(\boldsymbol{r},\boldsymbol{r})i\gamma_5\boldsymbol{\tau}\cdot\hat{\boldsymbol{r}}\;\; = \sin\Theta(r)\;\left\{{\rm tr}\int d\Omega\;\rho^S(\boldsymbol{r},\boldsymbol{r}) - \frac{4\pi}{N_C}\frac{m_\pi^2 f_\pi^2}{m}\right\} \tag{1.18}$$

where the traces are over flavor and Dirac indices only. According to the sum (1.14) the scalar quark density matrix $\rho^S(\boldsymbol{x},\boldsymbol{y})) = \langle q(\boldsymbol{x})\bar{q}(\boldsymbol{y})\rangle$ is decomposed into valence quark and Dirac sea parts:

$$\begin{aligned}
\rho^S(\boldsymbol{x},\boldsymbol{y}) &= \rho^S_{\rm val}(\boldsymbol{x},\boldsymbol{y}) + \rho^S_{\rm vac}(\boldsymbol{x},\boldsymbol{y}) \\
\rho^S_{\rm val}(\boldsymbol{x},\boldsymbol{y}) &= \sum_\nu \Psi_\nu(\boldsymbol{x})\eta_\nu\bar{\Psi}_\nu(\boldsymbol{y}){\rm sgn}(\epsilon_\nu) \\
\rho^S_{\rm vac}(\boldsymbol{x},\boldsymbol{y}) &= \frac{-1}{2}\sum_\nu \Psi_\nu(\boldsymbol{x}){\rm erfc}\left(\left|\frac{\epsilon_\nu}{\Lambda}\right|\right)\bar{\Psi}_\nu(\boldsymbol{y}){\rm sgn}(\epsilon_\nu).
\end{aligned} \tag{1.19}$$

For various boundary conditions the explicit form of the eigen–functions $\Psi_\nu(\boldsymbol{x})$ may *e.g.* be found in refs. [22, 23, 24]. Numerically the soliton is obtained iteratively. One starts off with a test profile $\Theta(r)$ which is employed to compute the eigenvalues and –states of h_0 (1.16). These are then substituted into the equation of motion (1.18) in order to update the profile function $\Theta(r)$. This procedure is repeated until convergence is reached.

[§]Here we attach the subscript "0" for later reference when fluctuations are included.

2. Mesonic Fluctuations off the Soliton

Mesonic fluctuations off the chiral soliton in the NJL model have been examined at length in the context of the bound state approach to the description of hyperons [25, 26, 27]. As the general formalism is not altered we will only point out the key steps and emphasize the changes due to the two flavor reduction.

Here we will only consider pseudoscalar fields and constrain the scalar fields to the chiral circle. Then a convenient parametrization for the fluctuations off the soliton is given by [25]

$$M(\boldsymbol{r},t) = m\ \xi_0(\boldsymbol{r})\xi_f(\boldsymbol{r},t)\xi_f(\boldsymbol{r},t)\xi_0(\boldsymbol{r}) \tag{2.1}$$

wherein $\xi_0(\boldsymbol{r})$ denotes static hedgehog configuartion (1.15) while $\xi_f(\boldsymbol{r},t)$ contains the small amplitude fluctuations $\boldsymbol{\eta}(\boldsymbol{r},t)$

$$\xi_f(\boldsymbol{r},t) = \exp\left(\frac{i}{2}\boldsymbol{\eta}(\boldsymbol{r},t)\cdot\boldsymbol{\tau}\right) = 1 + \frac{i}{2}\boldsymbol{\eta}(\boldsymbol{r},t)\cdot\boldsymbol{\tau} - \frac{1}{8}\boldsymbol{\eta}(\boldsymbol{r},t)\cdot\boldsymbol{\eta}(\boldsymbol{r},t) + \dots\ . \tag{2.2}$$

Subsequently the total action is expanded up to quadratic order in $\boldsymbol{\eta}(\boldsymbol{r},t)$. The zeroth order term just renders the static energy function which is explained in the introduction while the linear term vanishes subject to the stationary condition (1.18). The expression for the quadratic part has been derived in ref.[25]. In order to present that result it is useful to define the perturbation of the Dirac Hamiltonian

$$i\beta\not{D}_E = -\partial_\tau - h = -\partial_\tau - (h_0 + h_1 + h_2 + \dots) \tag{2.3}$$

wherein the subscript labels the power of the meson fluctuations. The zeroth order part is already presented in eqn (1.16). In order to display the linear and quadratic parts we make use of the unitary matrix [15, 28, 26]

$$\mathcal{T} = \xi_0 P_L + \xi_0^\dagger P_R \tag{2.4}$$

which contains the information about the static soliton. Then

$$h_1(\boldsymbol{r},-i\tau) = im\mathcal{T}\beta\gamma_5\boldsymbol{\eta}\cdot\boldsymbol{\tau}\mathcal{T}^\dagger \qquad \text{and} \qquad h_2(\boldsymbol{r},-i\tau) = -\frac{m}{2}\mathcal{T}\beta\boldsymbol{\eta}\cdot\boldsymbol{\eta}\mathcal{T}^\dagger. \tag{2.5}$$

Here it should be remarked that the temporal argument of the fluctuations is continued to Euclidean space, *i.e.* $\boldsymbol{\eta} = \boldsymbol{\eta}(\boldsymbol{r},-i\tau)$ The defining equation (2.3) is then employed to expand the operators $\not{D}_E^\dagger\not{D}_E$ and $\not{D}_E\left(\not{D}_E^\dagger\right)^{-1}$ up to quadratic order in $\boldsymbol{\eta}$. The resulting expression is subsequently substituted into eqns (1.6) and (1.5) for computing the contribution of the fermion determinant to the part of the action being quadratic in the fluctuations. At this point it is important to note that one is forced to start off the expansion at eqn (1.6) rather than employing standard perturbation techniques to the energy eigenvalues (1.10). The latter prescription would give incorrect results since $[\partial_\tau, h_{1,2}] \neq 0$. For the expansion in Euclidean space one Fourier–transforms the fluctuations

$$\eta_a(\boldsymbol{r},-i\tau) = \int_{-\infty}^{+\infty}\frac{d\omega_E}{2\pi}\tilde{\eta}_a(\boldsymbol{r},i\omega_E)\mathrm{e}^{-i\omega_E\tau}. \tag{2.6}$$

This transformation may be transferred to the Hamiltonian:

$$\begin{aligned} h_1(\boldsymbol{r},-i\tau) &= \int_{-\infty}^{+\infty}\frac{d\omega_E}{2\pi}\tilde{h}_{(1)}(\boldsymbol{r},i\omega_E)\mathrm{e}^{-i\omega_E\tau} \quad \text{and} \\ h_2(\boldsymbol{r},-i\tau) &= \int_{-\infty}^{+\infty}\frac{d\omega_E}{2\pi}\int_{-\infty}^{+\infty}\frac{d\omega'_E}{2\pi}\tilde{h}_{(2)}(\boldsymbol{r},i\omega_E,i\omega'_E)\mathrm{e}^{-i(\omega_E+\omega'_E)\tau} \end{aligned} \tag{2.7}$$

because $\mathcal{T}$ is static. The final expression for the harmonic part, $\mathcal{A}_2$, of the Euclidean action is then continued back to Minkowski space: $i\omega_E \to \omega$. The result may be expressed as a sum of three pieces

$$\mathcal{A}_2 = \mathcal{A}_{\rm val} + \mathcal{A}_{\rm vac} + \mathcal{A}_m. \tag{2.8}$$

The contribution due to the explicit occupation of the valence quark orbit ($|\mathrm{val}\rangle$) is given by

$$\begin{aligned} \mathcal{A}_{\rm val} &= -\eta^{\rm val}N_C\Big\{\int_{-\infty}^{+\infty}\frac{d\omega}{2\pi}\Big[\langle \mathrm{val}|\tilde{h}_2(\boldsymbol{r},\omega,-\omega)|\mathrm{val}\rangle \\ &\qquad + \sum_{\mu\neq\mathrm{val}}\langle \mathrm{val}|\tilde{h}_1(\boldsymbol{r},\omega)|\mu\rangle\langle\mu|\tilde{h}_1(\boldsymbol{r},-\omega)|\mathrm{val}\rangle\frac{\epsilon_{\rm val}-\epsilon_\mu}{(\epsilon_{\rm val}-\epsilon_\mu)^2-\omega^2}\Big]\Big\}. \end{aligned} \tag{2.9}$$

The contribution from the polarized Dirac sea is somewhat lengthy

$$\begin{aligned} \mathcal{A}_{\rm vac} &= \frac{N_C}{2}\int_{1/\Lambda^2}^{\infty}\frac{ds}{\sqrt{4\pi s}}\sum_\mu 2\epsilon_\mu \mathrm{e}^{-s\epsilon_\mu^2}\int_{-\infty}^{+\infty}\frac{d\omega}{2\pi}\langle\mu|\tilde{h}_2(\boldsymbol{r},\omega,-\omega)|\mu\rangle \\ &\quad + \frac{N_C}{4}\int_{1/\Lambda^2}^{\infty}ds\sqrt{\frac{s}{4\pi}}\sum_{\mu\nu}\int_{-\infty}^{+\infty}\frac{d\omega}{2\pi}\langle\mu|\tilde{h}_1(\boldsymbol{r},\omega)|\nu\rangle\langle\nu|\tilde{h}_1(\boldsymbol{r},-\omega)|\mu\rangle \\ &\qquad \times\left\{\frac{\mathrm{e}^{-s\epsilon_\mu^2}+\mathrm{e}^{-s\epsilon_\nu^2}}{s}+[\omega^2-(\epsilon_\mu+\epsilon_\nu)^2]R(s;\omega,\epsilon_\mu,\epsilon_\nu)\right\}. \end{aligned} \tag{2.10}$$

The regulator function R involves a Feynman parameter integral which reflects the quark loop in the presence of the soliton

$$R(s;\omega,\epsilon_\mu,\epsilon_\nu) = \int_0^1 dx\,\exp\left(-s[(1-x)\epsilon_\mu^2 + x\epsilon_\nu^2 - x(1-x)\omega^2]\right). \tag{2.11}$$

Here it should be noted that, upon explicit calculation, it can be shown that the matrix elements $\langle\mu|\tilde{h}_2(\boldsymbol{r},\omega,-\omega)|\mu\rangle$ and $\langle\mu|\tilde{h}_1(\boldsymbol{r},\omega)|\nu\rangle\langle\nu|\tilde{h}_1(\boldsymbol{r},-\omega)|\mu\rangle$ are invariant under $\omega\to-\omega$. This is the reason why the terms of odd powers in ω have been dropped in the eqns (2.9,2.10). Stated otherwise: The imaginary part of the action does not contribute in the two flavor reduction contrary to the case when strange degrees of freedom are present [25, 26]. Finally the action is completed by the mesonic part

$$\mathcal{A}_m = -\frac{m_\pi^2 f_\pi^2}{2}\int d^3r\int_{-\infty}^{+\infty}\frac{d\omega}{2\pi}\,\cos\Theta\;\tilde{\boldsymbol{\eta}}(\boldsymbol{r},\omega)\cdot\tilde{\boldsymbol{\eta}}(\boldsymbol{r},-\omega). \tag{2.12}$$

Formally the harmonic part of the action can be expressed with the help of local $\Phi_1^{ab}(\boldsymbol{r})$ and bilocal $\Phi_2^{ab}(\boldsymbol{r},\boldsymbol{r}',\omega)$ kernels

$$\begin{aligned} \mathcal{A}_2 &= \frac{1}{2}\int_{-\infty}^{+\infty}\frac{d\omega}{2\pi}\Big\{\int d^3r\int d^3r'\Phi_2^{ab}(\boldsymbol{r},\boldsymbol{r}',\omega)\tilde{\eta}_a(\boldsymbol{r},\omega)\tilde{\eta}_b(\boldsymbol{r}',-\omega) \\ &\qquad + \int d^3r\Phi_1^{ab}(\boldsymbol{r})\tilde{\eta}_a(\boldsymbol{r},\omega)\tilde{\eta}_b(\boldsymbol{r},-\omega)\Big\}. \end{aligned} \tag{2.13}$$

These kernels can be extracted from the above expressions. The local kernel turns out to be diagonal in isospace $\Phi_1^{ab}(\boldsymbol{r}) = \Phi_1(\boldsymbol{r})\delta^{ab}$. Here we recognize the usefulness of the above defined unitary matrix $\mathcal{T}$ (2.4) because it considerably simplifies the presentation of these kernels by defining chirally rotated wave–functions $\tilde{\Psi}_\mu = \mathcal{T}^\dagger \Psi_\mu$. Then we find

$$\begin{aligned}\Phi_1(\boldsymbol{r}) &= -m_\pi^2 f_\pi^2 \cos\Theta(r) + 2\eta_{\rm val} N_C m \tilde{\Psi}^\dagger_{\rm val}(\boldsymbol{r})\beta\tilde{\Psi}_{\rm val}(\boldsymbol{r}) \\ &\quad -2N_C m \int_{1/\Lambda^2}^\infty \frac{ds}{\sqrt{4\pi s}} \sum_\mu \epsilon_\mu e^{-s\epsilon_\mu^2} \tilde{\Psi}^\dagger_\mu(\boldsymbol{r})\beta\tilde{\Psi}_\mu(\boldsymbol{r}) \qquad (2.14)\end{aligned}$$

and

$$\begin{aligned}\Phi_2^{ab}(\boldsymbol{r},\boldsymbol{r}',\omega) &= 2\eta_{\rm val} N_C m^2 \sum_{\mu\neq{\rm val}} \tilde{\Psi}^\dagger_{\rm val}(\boldsymbol{r})\beta\gamma_5\tau^a\tilde{\Psi}_\mu(\boldsymbol{r})\tilde{\Psi}^\dagger_\mu(\boldsymbol{r}')\beta\gamma_5\tau^b\tilde{\Psi}_{\rm val}(\boldsymbol{r}')\frac{\epsilon_{\rm val}-\epsilon_\mu}{(\epsilon_{\rm val}-\epsilon_\mu)^2-\omega^2} \\ &\quad -\frac{N_C}{2}m^2\int_{1/\Lambda^2}^\infty ds\sqrt{\frac{s}{4\pi}}\sum_{\mu\nu}\tilde{\Psi}^\dagger_\nu(\boldsymbol{r})\beta\gamma_5\tau^a\tilde{\Psi}_\mu(\boldsymbol{r})\tilde{\Psi}^\dagger_\mu(\boldsymbol{r}')\beta\gamma_5\tau^b\tilde{\Psi}_\nu(\boldsymbol{r}') \\ &\quad \times\left\{\frac{{\rm e}^{-s\epsilon_\mu^2}+{\rm e}^{-s\epsilon_\nu^2}}{s}+[\omega^2-(\epsilon_\mu+\epsilon_\nu)^2]R(s;\omega,\epsilon_\mu,\epsilon_\nu)\right\}. \qquad (2.15)\end{aligned}$$

In ref.[26] it has been demonstrated that these kernels are diagonal in parity and grand spin, *i.e.* meson fluctuations with different grand spin and/or parity quantum numbers decouple. This is a consequence of the fact that the classical soliton carries zero grand spin and has definite parity. This decoupling of the meson fluctuations will later on be helpful since it allows us to consider rotational and translational zero modes separately. The equation of motion for the fluctuations is finally obtained by varying (2.13) with respect to $\tilde{\eta}_a(\boldsymbol{r},\omega)$

$$\int d^3r'\ \Phi_2^{ab}(\boldsymbol{r},\boldsymbol{r}',\omega)\tilde{\eta}_b(\boldsymbol{r}',\omega) + \Phi_1(\boldsymbol{r})\tilde{\eta}_a(\boldsymbol{r},\omega) = 0 \qquad (2.16)$$

which in fact represents the Bethe–Salpeter equation for the pion fluctuations in the soliton background. This equation has the following interpretation: The frequency ω has to be adjusted to ω_i such that (2.16) is satisfied for a non–trivial $\tilde{\eta}_a(\boldsymbol{r},\omega_i)$. The frequency ω_i is called eigen–frequency and $\tilde{\eta}_a(\boldsymbol{r},\omega_i)$ denotes the associated eigen–mode or –wave–function. Below we will explain how the boundary conditions, which are imposed on the Dirac spinors Ψ_ν, transfer to the meson fluctuations and subsequently lead to a discrete meson spectrum as well. The numerical methods which are used to solve eqn (2.16) are reported in refs.[29, 30].

Later on we will have to evaluate overlap matrix elements between the solutions to the Bethe–Salpeter eqn (2.16) and states which solve this equation in the absence of the soliton *i.e.* $\Theta \equiv 0$. The latter states are obtained by computing the above defined kernels Φ_1 and Φ_2 as mode sums which contain the eigenvalues and –states of the free Dirac Hamiltonian

$$h_{\rm free} = \boldsymbol{\alpha}\cdot\boldsymbol{p} + \beta m. \qquad (2.17)$$

Let us denote the resulting kernels by $\Phi_{1,2}^{ab(0)}$ and the solutions to the corresponding Bethe–Salpeter equation by $\tilde{\boldsymbol{\eta}}^{(0)}(\boldsymbol{r},\omega_i^{(0)})$. Of course, the eigen–frequencies $\omega_i^{(0)}$ will differ from those obtained in the presence of the soliton. It should be remarked that $\tilde{\boldsymbol{\eta}}^{(0)}(\boldsymbol{r},\omega_i^{(0)})$ do not necessarily solve a Klein–Gordon equation due to the composite nature of our meson fields.

In the first place we therefore have to find the proper normalization of the solutions to eqn (2.16). In the case of the NJL model this turns out to be more involved than *e.g.* for the Skyrme model because the the frequency ω appears with all even powers in eqn (2.16) rather than only quadratically. Therefore the metric which appears in the scalar product of the underlying Hilbert space of the fluctuations unavoidably depends on the frequency. In order to compute this metric we (formally) expand the Bethe–Salpeter equation (2.16) in terms of the frequency

$$\sum_{n=0}^{\infty} \int d^3r' \mathcal{O}_n^{ab}(\boldsymbol{r},\boldsymbol{r}') \omega_i^{2n} \tilde{\eta}_b(\boldsymbol{r}',\omega_i) = 0 \tag{2.18}$$

and assume that $\tilde{\eta}_a(\boldsymbol{r},\omega_i)$ represents an eigen–mode with frequency ω_i. The expansion (2.18) obviously represents a generalization to the free Klein–Gordon equation which corresponds to $\mathcal{O}_0 = -m_\pi^2 - \boldsymbol{\partial}^2$ and $\mathcal{O}_1 = 1$ while all other $\mathcal{O}_n$ vanish. Also in the Skyrme model only $\mathcal{O}_0$ and $\mathcal{O}_1$ are non–zero. As compared to the Klein–Gordon equation, however, they acquire additional space dependent factors.

For the general case we start with the identity

$$0 = \int d^3r \int d^3r' \tilde{\eta}_a(\boldsymbol{r},\omega_i) \left[\mathcal{O}_0^{ab}(\boldsymbol{r},\boldsymbol{r}') - \mathcal{O}_0^{ab}(\boldsymbol{r},\boldsymbol{r}')\right] \tilde{\eta}_b(\boldsymbol{r}',\omega_j). \tag{2.19}$$

Noting that the $\mathcal{O}_n^{ab}$ are Hermitian under the spatial integration we obtain by substituting the Bethe–Salpeter equation (2.18)

$$0 = \int d^3r \int d^3r' \sum_{n=1}^{\infty} \tilde{\eta}_a(\boldsymbol{r},\omega_i) \mathcal{O}_n^{ab}(\boldsymbol{r},\boldsymbol{r}') \left[\omega_j^{2n} - \omega_i^{2n}\right] \tilde{\eta}_b(\boldsymbol{r}',\omega_j) \tag{2.20}$$

$$= \left(\omega_j^2 - \omega_i^2\right) \int d^3r \int d^3r' \tilde{\eta}_a(\boldsymbol{r},\omega_i) \left[\sum_{n=1}^{\infty} \mathcal{O}_n^{ab}(\boldsymbol{r},\boldsymbol{r}') \sum_{p=0}^{n-1} \omega_j^{2p} \omega_i^{2(n-1-p)}\right] \tilde{\eta}_b(\boldsymbol{r}',\omega_j). \tag{2.21}$$

Here the relation $a^n - b^n = (a-b)\sum_{m=0}^{n-1} a^m b^{(n-1-m)}$ has been used. Eqn (2.21) allows one to impose the orthonormalization condition

$$\int d^3r \int d^3r' \tilde{\eta}_a(\boldsymbol{r},\omega_i) \left[\sum_{n=1}^{\infty} \mathcal{O}_n^{ab}(\boldsymbol{r},\boldsymbol{r}') \sum_{p=0}^{n-1} \omega_j^{2p} \omega_i^{2(n-1-p)}\right] \tilde{\eta}_b(\boldsymbol{r}',\omega_j) = \delta_{ij}. \tag{2.22}$$

In particular a solution $\tilde{\eta}_a(\boldsymbol{r},\omega_i)$ to the Bethe–Salpeter equation is normalized to

$$\int d^3r \int d^3r' \tilde{\eta}_a(\boldsymbol{r},\omega_i) \mathcal{M}^{ab}(\boldsymbol{r},\boldsymbol{r}',\omega_i) \tilde{\eta}_b(\boldsymbol{r}',\omega_i) = 1 \tag{2.23}$$

which defines the metric tensor

$$\begin{aligned} \mathcal{M}^{ab}(\boldsymbol{r},\boldsymbol{r}',\omega_i) &= \sum_{n=1}^{\infty} \mathcal{O}_n^{ab}(\boldsymbol{r},\boldsymbol{r}') \sum_{p=0}^{n-1} \omega_i^{2p} \omega_i^{2(n-1-p)} = \sum_{n=1}^{\infty} n\, \omega_i^{2(n-1)} \mathcal{O}_n^{ab}(\boldsymbol{r},\boldsymbol{r}') \\ &= \left.\frac{\partial \Phi_2^{ab}(\boldsymbol{r},\boldsymbol{r}',\omega)}{\partial \omega^2}\right|_{\omega=\omega_i}. \end{aligned} \tag{2.24}$$

As a matter of fact this metric tensor can easily be obtained from eqn (2.15) in contrast to the expansion coefficients $\mathcal{O}_n^{ab}$. We have thus succeeded in deriving a normalization

condition for the solutions to the Bethe–Salpeter equation in the soliton background. This represents a special achievement because in the Bethe–Salpeter equation the frequency ω appears with arbitrary even powers. In coordinate space these are time derivatives.

As we will take advantage of the grand spin symmetry when computing overlaps between $\tilde{\boldsymbol{\eta}}$ and $\tilde{\boldsymbol{\eta}}^{(0)}$ it is appropriate to also define a metric tensor $\mathcal{M}_i^{ab(0)}(\boldsymbol{r},\boldsymbol{r}',\omega_i^{(0)})$ for the fluctuations in the baryon number zero sector. This quantity is obtained by substituting $\Phi_2^{ab(0)}$ in eqn (2.24).

Now we are finally enabled to equip the overlap $\langle\tilde{\boldsymbol{\eta}}(\boldsymbol{r},\omega_i)|\tilde{\boldsymbol{\eta}}^{(0)}(\boldsymbol{r},\omega_j^{(0)})\rangle$ with an ingenious meaning. To do so we first redefine the meson wave–functions $\tilde{\boldsymbol{\eta}} \to \tilde{\boldsymbol{\phi}}$ such that they are normalized to unity with respect to the trivial metric

$$\int d^3r \boldsymbol{\phi}(\boldsymbol{r},\omega_i)\cdot\boldsymbol{\phi}(\boldsymbol{r},\omega_i) = 1. \tag{2.25}$$

This can obviously be achieved by the introduction of the root [31] (see section 4 for its explicit construction)

$$\mathcal{M}^{ab}(\boldsymbol{r},\boldsymbol{r}',\omega_i) = \int d^3x \sum_{c=1}^{3} \left(\sqrt{\mathcal{M}}\right)^{ac}(\boldsymbol{r},\boldsymbol{x},\omega_i)\ \left(\sqrt{\mathcal{M}}\right)^{bc}(\boldsymbol{r}',\boldsymbol{x},\omega_i) \tag{2.26}$$

into the wave–function

$$\phi^a(\boldsymbol{r},\omega_i) = \int d^3x \sum_{c=1}^{3} \left(\sqrt{\mathcal{M}}\right)^{ca}(\boldsymbol{x},\boldsymbol{r},\omega_i)\ \tilde{\eta}_c(\boldsymbol{x},\omega_i). \tag{2.27}$$

The application of these definitions to the baryon number zero sector is straightforward yielding $\boldsymbol{\phi}^{(0)}(\boldsymbol{r},\omega_j^{(0)})$. To this end the above mentioned matrix element is defined as

$$\langle\tilde{\boldsymbol{\eta}}(\boldsymbol{r},\omega_i)|\tilde{\boldsymbol{\eta}}^{(0)}(\boldsymbol{r},\omega_j^{(0)})\rangle := \int d^3r\ \boldsymbol{\phi}(\boldsymbol{r},\omega_i)\cdot\boldsymbol{\phi}^{(0)}(\boldsymbol{r},\omega_j^{(0)}). \tag{2.28}$$

This actually is the generalization of the Skyrme model definition for this overlap [14] in the case that the metric in the orthogonality condition (2.22) depends on the frequencies of the states. It should, however, be noted that this procedure only yields normalized wave–functions and that there does not exist an orthogonality condition for the fluctuations $\boldsymbol{\phi}(\boldsymbol{r},\omega_i)$. Nevertheless the definition (2.28) represents the most reasonable one because the wave–functions $\tilde{\boldsymbol{\eta}}$ and $\tilde{\boldsymbol{\eta}}^{(0)}$ obey Bethe–Salpeter equations which in principle are disconnected because they belong to different baryon sectors and thus different Hilbert spaces.

There is one more important point which has to be mentioned in the context of the Bethe–Salpeter equation for the meson fluctuations in the NJL model. As this stems from a shortcoming of the NJL model in general it effects the eigen–modes in the presence as well as in absence of the soliton. The NJL model is well known not to possess quark confinement. Thus meson fields may decay into "free" quark–antiquark pairs once the meson energy ω is beyond the two quark threshold $\omega_{\text{thres}}^{(0)} = 2m$. Technically this appears because the argument of the exponent in Feynman parameter integral (2.11) turns negative. As a matter of fact the analytic continuation from Euclidean to Minkowski space yielding eqn (2.10) is ill–defined for $\omega^{(0)} \geq \omega_{\text{thres}}^{(0)}$. Along this path in the complex plane the logarithm develops an imaginary part which measures the width for the meson to decay into a quark–antiquark pair. Therefore the expansion of $\Phi_2^{ab(0)}$ which finally yielded $\mathcal{M}_i^{ab(0)}$

converges only for $\omega^{(0)} \leq 2m$. Later on we will have to perform sums over the eigen–modes $\tilde{\eta}^{(0)}(\boldsymbol{r}, \omega_i^{(0)})$. As a consequence of these considerations, $\omega_{\rm thres}^{(0)}$ provides a natural cut–off to these mode sums. In the presence of the soliton the situation is even worse because the valence quark orbit gets bound and acquires an energy eigenvalue $\epsilon_{\rm val} < m$. Following the analysis presented in appendix B of ref.[27] this leads to the threshold $\omega_{\rm thres} = 2|\epsilon_{\rm val}| < 2m$. Fortunately, this threshold will not be of utmost relevance for the ongoing studies because we are mostly interested in the zero modes ($\omega_i = 0$) in the soliton background.

3. Energy Functional for Fluctuations

In order to compute the quantum corrections to the soliton mass we first have to construct the energy functional for the meson fluctuations. Again this is not straightforward because the Bethe–Salpeter equation involves arbitrary even powers of the frequency ω. We therefore have to go back to the expansion (2.18) of the Bethe–Salpeter equation. Formally the Bethe–Salpeter equation is obtained from the action formulated in Fourier space

$$S[\tilde{\boldsymbol{\eta}}] = \frac{1}{2} \int \frac{d\omega}{2\pi} \int d^3r \int d^3r' \tilde{\eta}_a(\boldsymbol{r}, -\omega) \left[\sum_{n=0}^{\infty} \mathcal{O}_n^{ab}(\boldsymbol{r}, \boldsymbol{r}') \omega^{2n} \right] \tilde{\eta}_b(\boldsymbol{r}', \omega). \tag{3.1}$$

Undoing the Fourier transformation one obtains the Lagrange function

$$L = \frac{1}{2} \int d^3r \int d^3r' \sum_{n=0}^{\infty} \eta_a^{(n)}(\boldsymbol{r}, t) \mathcal{O}_n^{ab}(\boldsymbol{r}, \boldsymbol{r}') \eta_b^{(n)}(\boldsymbol{r}', t) \tag{3.2}$$

where the superscript denotes the order of the time derivative of the fluctuation $\eta_a(\boldsymbol{r}, t)$. As in classical mechanics we compute the total derivative of L with respect to the time coordinate in order to derive the conserved energy. Upon integration by parts we find

$$\begin{aligned} \frac{d}{dt} L &= \sum_{n=0}^{\infty} \int d^3r \left\{ \frac{d}{dt} \Big[\sum_{m=0}^{n} (-1)^m \eta_a^{(n-m)}(\boldsymbol{r}, t) \left(\frac{\partial^m}{\partial t^m} \right) \frac{\delta L}{\delta \eta_a^{(n)}(\boldsymbol{r}, t)} \Big] \right. \\ &\qquad \left. + (-1)^n \eta_a^{(n)}(\boldsymbol{r}, t) \left(\frac{\partial^n}{\partial t^n} \right) \frac{\delta L}{\delta \eta_a^{(n)}(\boldsymbol{r}, t)} \right\}. \end{aligned} \tag{3.3}$$

Inserting the expansion (3.2) and the Fourier–transformation for the fluctuations (2.6) the last, *i.e.* surface term in (3.3) is shown to vanish for meson fields which satisfy the Bethe–Salpeter equation (2.16,2.18). Thus the conserved quantity which has to be identified as the energy functional and thus the Hamiltonian is given by

$$\begin{aligned} \mathcal{H}[\boldsymbol{\eta}] &= \int d^3r \left\{ \sum_{n=0}^{\infty} \sum_{m=0}^{n} (-1)^m \eta_a^{(n-m)}(\boldsymbol{r}, t) \left(\frac{\partial^m}{\partial t^m} \right) \frac{\delta L}{\delta \eta_a^{(n)}(\boldsymbol{r}, t)} \right\} - L \\ &= \int d^3r \int d^3r' \left\{ \sum_{n=0}^{\infty} \sum_{m=0}^{n} (-1)^m \eta_a^{(n-m)}(\boldsymbol{r}, t) \mathcal{O}_n^{ab}(\boldsymbol{r}, \boldsymbol{r}') \eta_b^{(n+m)}(\boldsymbol{r}', t) \right. \\ &\qquad \left. - \frac{1}{2} \sum_{m=0}^{n} \eta_a^{(n)}(\boldsymbol{r}, t) \mathcal{O}_n^{ab}(\boldsymbol{r}, \boldsymbol{r}') \eta_b^{(n)}(\boldsymbol{r}', t) \right\}. \end{aligned} \tag{3.4}$$

Next the fluctuating field $\boldsymbol{\eta}(\boldsymbol{r}, t)$ is decomposed in terms of the solutions to the Bethe–Salpeter equation (2.16)

$$\boldsymbol{\eta}(\boldsymbol{r}, t) = \sum_i \frac{1}{\sqrt{2\omega_i}} \left\{ a_i \tilde{\boldsymbol{\eta}}(\boldsymbol{r}, \omega_i) e^{i\omega_i t} + a_i^\dagger \tilde{\boldsymbol{\eta}}(\boldsymbol{r}, \omega_i) e^{-i\omega_i t} \right\} \tag{3.5}$$

because the solutions to (2.16) come in pairs $\pm\omega_i$, *i.e.* $\boldsymbol{\eta}(\boldsymbol{r},t)$ describes a real field. The canonical quantization prescription then corresponds to require the commutation relations

$$\left[a_i, a_j^\dagger\right] = \delta_{ij}. \tag{3.6}$$

The decomposition (3.5) is substituted into the energy functional for the meson fluctuations (3.4). The aim is then to obtain an expression in terms of the operators a_i and $a_i^\dagger$ by using the orthonormalization condition (2.22). It is obvious that at an intermediate step the term involving $\mathcal{O}_0^{ab}$ has to be eliminated. This is done in a symmetric way by the help of the Bethe–Salpeter equation

$$\begin{aligned}\int d^3r \int d^3r'\ \tilde{\eta}_a(\boldsymbol{r},\omega_i)\mathcal{O}_0^{ab}(\boldsymbol{r},\boldsymbol{r}')\tilde{\eta}_b(\boldsymbol{r}',\omega_j) = \\ -\frac{1}{2}\int d^3r \int d^3r'\ \tilde{\eta}_a(\boldsymbol{r},\omega_i)\left[\sum_{n=1}^{\infty}\left(\omega_i^{2n}+\omega_j^{2n}\right)\mathcal{O}_n^{ab}(\boldsymbol{r},\boldsymbol{r}')\tilde{\eta}_b(\boldsymbol{r}',\omega_j)\right].\end{aligned} \tag{3.7}$$

After a somewhat tedious calculation we find

$$\begin{aligned}\mathcal{H} \;=\; & \frac{1}{2}\sum_i \omega_i \int d^3r \int d^3r'\ \tilde{\eta}_a(\boldsymbol{r},\omega_i)\left[\sum_{n=1}^{\infty} n\ \omega_i^{2(n-1)}\mathcal{O}_n^{ab}(\boldsymbol{r},\boldsymbol{r}')\right]\tilde{\eta}_b(\boldsymbol{r}',\omega_i) \\ & + \sum_{ij}\frac{1}{\sqrt{4\omega_i\omega_j}}\int d^3r \int d^3r'\ \tilde{\eta}_a(\boldsymbol{r},\omega_i)\left[\sum_{n=1}^{\infty}\sum_{m=0}^{n-1}\omega_i^{2m}\omega_j^{2(n-m-1)}\mathcal{O}_n^{ab}(\boldsymbol{r},\boldsymbol{r}')\right]\tilde{\eta}_b(\boldsymbol{r}',\omega_j) \\ & \times\left[\frac{a_i a_j}{4}\left(\omega_i-\omega_j\right)^2 e^{i(\omega_i+\omega_j)t} + \frac{a_i^\dagger a_j^\dagger}{4}\left(\omega_i-\omega_j\right)^2 e^{-i(\omega_i+\omega_j)t}\right. \\ & \left. + \frac{a_i^\dagger a_j}{2}\left(\omega_i+\omega_j\right)^2 e^{-i(\omega_i-\omega_j)t}\right].\end{aligned} \tag{3.8}$$

Here we finally recognize the appearance of the orthonormalization condition (2.22). Hence we arrive at the energy operator of an harmonic oscillator

$$\mathcal{H} = \sum_i \omega_i\left(a_i^\dagger a_i + \frac{1}{2}\right). \tag{3.9}$$

Although this result is not unexpected it is at the same time non–trivial because the Bethe–Salpeter equation (2.16), which is the defining equation for the normal modes of energy ω_i, contains arbitrary even powers of the time derivative operator when transformed to coordinate space. Needless to mention that the above analysis goes through as well in the absence of the soliton resulting in

$$\mathcal{H}^{(0)} = \sum_i \omega_i^{(0)}\left(a_i^{(0)\dagger} a_i^{(0)} + \frac{1}{2}\right). \tag{3.10}$$

Here $a_i^{(0)\dagger}$ and $a_i^{(0)}$ respectively denote the creation and annihilation operators for the eigen–modes $\tilde{\boldsymbol{\eta}}^{(0)}(\boldsymbol{r},\omega_i^{(0)})$.

We have thus seen that the vacuum energy, $\sum_i \omega_i/2$, corresponds to the one of an harmonic oscillator and that this result is independent of the specific form of the kernel for the Bethe–Salpeter equation. There are two restrictions only:

(i) The eigenvalues appear in pairs $\pm\omega_i$.

(ii) The background field is static.

In order to see that the vacuum contribution to the Hamiltonian (3.9) comes with no surprise but rather is a feature of the semi–classical treatment of the meson fluctuations we read off the inverse propagator for these fluctuations from the action (3.1)

$$\left(\mathcal{D}^{-1}\right)^{ab}(\boldsymbol{r},\boldsymbol{r}',\omega^2) = \sum_{n=0}^{\infty} \mathcal{O}_n^{ab}(\boldsymbol{r},\boldsymbol{r}')\omega^{2n}. \tag{3.11}$$

Since the background field is static the propagator $\mathcal{D}$ is local rather than bilocal in the frequency ω.

In order to extract the vacuum contribution of the meson fluctuations in the soliton background in the semi–classical approximation one considers the functional integral (continued to Euclidean space)

$$e^{-\mathcal{A}_M} = \int D\tilde{\eta}\, \exp\left\{-S_E[\tilde{\eta}]\right\} = \left[\mathrm{Det}\left(\mathcal{D}^{-1}\right)\right]^{-\frac{1}{2}}, \tag{3.12}$$

i.e.

$$\mathcal{A}_M = \frac{1}{2}\ \mathrm{Tr}\ \log\left(\mathcal{D}^{-1}\right). \tag{3.13}$$

The temporal part of the functional trace can be done because the propagator is local in the frequency. As in the case for the fermion determinant (*cf.* section 2) the vacuum part is obtained by considering the limit of infinitely large Euclidean times T. Then the temporal part of the trace becomes a spectral integral

$$\mathcal{A}_M = \frac{T}{2}\int_{-\infty}^{\infty}\frac{d\omega}{2\pi}\ Tr\ \log\left(\mathcal{D}^{-1}(\omega^2)\right) \tag{3.14}$$

where we have suppressed spatial and isospin arguments. Furthermore Tr refers to the trace over all degrees of freedom other than the time coordinate. Next we integrate by parts

$$\mathcal{A}_M = -\frac{T}{2}\int_{-\infty}^{\infty}\frac{d\omega}{2\pi}\ Tr\ \left(2\omega^2\mathcal{D}(\omega^2)\frac{\partial}{\partial\omega^2}\mathcal{D}^{-1}(\omega^2)\right). \tag{3.15}$$

The surface term has disappeared since the propagator only depends on ω^2. The trace Tr can be evaluated with the help of the solutions to the Bethe–Salpeter equation $\tilde{\boldsymbol{\eta}}(\boldsymbol{r},\omega_i)$

$$\mathcal{A}_M = \frac{T}{2}\int_{-\infty}^{\infty}\frac{d\omega}{2\pi}\ 2\omega^2\sum_i \langle i|\mathcal{D}(\omega^2)\frac{\partial}{\partial\omega^2}\mathcal{D}^{-1}(\omega^2)|i\rangle. \tag{3.16}$$

Now it is important to note that the states $|i\rangle$ represent the solutions to the Bethe–Salpeter equation. This allows one to expand

$$\langle i|\mathcal{D}(\omega^2) = \frac{1}{\omega^2-\omega_i^2}\left\{\frac{\partial}{\partial\omega^2}\langle i|\mathcal{D}^{-1}(\omega^2)\Big|_{\omega=\omega_i} + \mathcal{O}\left(\omega^2-\omega_i^2\right)\right\}^{-1}. \tag{3.17}$$

Hence

$$\mathcal{A}_M = -\frac{T}{2}\int\frac{d\omega}{2\pi}\sum_i\frac{2\omega^2}{\omega^2-\omega_i^2} \times\langle i|\left\{\frac{\partial}{\partial\omega^2}\mathcal{D}^{-1}(\omega^2)\Big|_{\omega=\omega_i}+\mathcal{O}\left(\omega^2-\omega_i^2\right)\right\}^{-1}\frac{\partial}{\partial\omega^2}\mathcal{D}^{-1}(\omega^2)|i\rangle. \quad (3.18)$$

Under the assumption that summation and integration may be exchanged the spectral integral may be computed with the help of the residue theorem

$$\begin{aligned}\mathcal{A}_M &= -\frac{T}{2}\sum_i\lim_{\omega\to\omega_i}(\omega-\omega_i)\frac{2\omega^2}{\omega^2-\omega_i^2}\langle i|\left\{\frac{\partial}{\partial\omega^2}\mathcal{D}^{-1}(\omega^2)\Big|_{\omega=\omega_i}\right\}^{-1}\frac{\partial}{\partial\omega^2}\mathcal{D}^{-1}(\omega^2)|i\rangle \\ &= -\frac{T}{2}\sum_i\omega_i. \end{aligned} \quad (3.19)$$

Thus we have seen on the formal level that the above listed restrictions to the Bethe–Salpeter equation are sufficient to provide a vacuum energy which is given by a sum of eigenfrequencies. However, the above derivation has to be taken with some care because the functional traces are, of course, divergent and thus require regularization as do the expressions (3.9) and (3.10). This issue will be discussed next.

The main content of the above considerations is indeed the fact that we have obtained a quantized Hamiltonian for the meson fluctuations which are formally equivalent to a harmonic oscillator. Considering eqn (3.19) one might be tempted to identify the quantum corrections to the energy as the difference

$$\frac{1}{2}\sum_i\omega_i-\frac{1}{2}\sum_j\omega_j^{(0)}.$$

However, this expression diverges logarithmically. In the context of the Skyrme model Holzwarth has shown that two additional subtractions yield a finite (renormalized) result [14]. To identify these subtractions in the NJL model we make use of the fact that eqns (3.9) and (3.10) imply the existence of operators H^2 and H_0^2 which have the eigenvalues ω_i^2 and $\omega_i^{(0)2}$ when acting on the meson eigen–modes in the baryon number one and zero sector, respectively. One may especially define the "perturbation potential" V via

$$H^2=H_0^2+V. \quad (3.20)$$

A finite expression for the vacuum energy is obtained after subtracting the first three terms in the expansion

$$Tr\left(\sqrt{H_0^2+V}\right)=Tr\left(H_0\right)+\frac{1}{2}Tr\left(H_0^{-1}V\right)-\frac{1}{8}Tr\left(H_0^{-1}VH_0^{-2}V\right)+\ldots \quad (3.21)$$

resulting in the finite energy correction due to the quantum fluctuations [14]

$$\triangle E=\frac{1}{2}Tr\left(H-H_0-\frac{1}{2}H_0^{-1}V+\frac{1}{8}H_0^{-3}V^2\right). \quad (3.22)$$

This expression, which was derived by Holzwarth in the case of the Skyrme model, represents the actual starting point of our investigations in the context of the NJL model. The

main complication in comparison with the Skyrme model is that we do not have explicit access to the operators H and H_0. However, we are able to compute the associated energy eigenvalues by solving the Bethe–Salpeter equation (2.16). Furthermore we have a suitable definition (2.28) for the overlap of the eigenstates of H and H_0. The energy correction (3.22) actually represents the $3+1$ dimensional generalization of the result obtained by Cahill, Comtet and Glauber [32] in a $1+1$ dimensional model. It should, however, be noted that the correction (3.22) is not free of ordering ambiguities.

As already mentioned we have access to the eigenvalues of H and H_0 only. Then the correction (3.22) may be expressed as

$$\begin{aligned} \triangle E &= \frac{1}{2}\sum_i \Bigg\{ \omega_i - \frac{1}{8}\sum_j \omega_j^{(0)} \left| \langle \tilde{\boldsymbol{\eta}}(\boldsymbol{r},\omega_i) | \tilde{\boldsymbol{\eta}}^{(0)}(\boldsymbol{r},\omega_j^{(0)}) \rangle \right|^2 \\ &\qquad \times \left[3 + 6\left(\frac{\omega_i}{\omega_j^{(0)}}\right)^2 - \left(\frac{\omega_i}{\omega_j^{(0)}}\right)^4 \right] \Bigg\}. \end{aligned} \tag{3.23}$$

Here the overlap $\langle \tilde{\boldsymbol{\eta}}(\boldsymbol{r},\omega_i) | \tilde{\boldsymbol{\eta}}^{(0)}(\boldsymbol{r},\omega_j^{(0)}) \rangle$ shows up since the trace has to be performed in a common Hilbert space to chop off both frequency sums in the same way. At this point it should also have become clear that the formal considerations in section 2 on the orthonormalization of the solutions to the Bethe–Salpeter equation are in fact unavoidable. Eqn (3.23) obviously yields $\triangle E = 0$ in the absence of the soliton, *i.e.* when $\omega_i = \omega_i^{(0)}$ and $\tilde{\boldsymbol{\eta}}(\boldsymbol{r},\omega_i) = \tilde{\boldsymbol{\eta}}^{(0)}(\boldsymbol{r},\omega_i^{(0)})$. We furthermore observe from eqn (3.23) that $\triangle E$ is of the order N_C^0 in agreement with the assertions made in the introduction.

From eqn (3.23) it is obvious that the zero modes, *i.e.* states with $\omega_i = 0$ may lead to a sizable reduction of the total energy $E + \triangle E$ since for these states $\triangle E$ is negative. The fact that for scattering states $\omega_i \approx \omega_i^{(0)}$ demonstrates that the main contributions to the quantum corrections is indeed due to the existence of zero modes in the soliton background. This can also be understood in the context of the phase–shift $\delta(k)$ expression for the Casimir energy, $E_{\rm cas} \sim (-1/2\pi)\int dk \delta(k)$ up to counterterms which render this integral finite for $k \to \infty$ [33]. According to Levison's theorem an additional π has to be included for each bound state. The only bound states in the background of the NJL soliton are the zero modes. Thus the channels in which these modes appear may considerably contribute to $E_{\rm cas}$. In the proceeding section we will therefore concentrate on the channels which contain the zero modes in the NJL model.

4. Zero Mode Channels

Zero modes, *i.e.* solutions to the Bethe–Salpeter equation (2.16) with $\omega_i = 0$, arise whenever the stationary background field (the "vacuum" seen by the meson fluctuations) breaks a symmetry of the underlying theory. In that sense the zero modes are Goldstone bosons. In the case of the chiral soliton the hedgehog field configuration (1.15) violates the rotational and translational invariance. We therefore expect zero modes to be associated with infinitesimal spatial rotations and translations of the soliton. Due to the grand spin symmetry the zero mode corresponding to infinitesimal iso–rotations is equivalent to the one of the spatial rotations. Although the model is invariant under axial rotations (for massless pions) a corresponding zero mode does not exist since the infinitesimal axial rotation does not leave the vacuum configuration ($M = m$) invariant.

In order to identify the zero modes we expand the parametrization (2.1) up to linear order in $\boldsymbol{\eta}(\boldsymbol{r},t)$

$$M = m\left\{\xi_0^2 + i\xi_0\boldsymbol{\eta}\cdot\boldsymbol{\tau}\xi_0\right\} + \ldots = M_0 + im\xi_0\boldsymbol{\eta}\cdot\boldsymbol{\tau}\xi_0 + \ldots \quad . \tag{4.1}$$

For the extraction of the formal structure of the zero modes we have to identify the linear term with $[\mathcal{G}, M_0]$. Here $\mathcal{G}$ refers to the generator of the symmetry transformation. For the spatial rotation this gives

$$\boldsymbol{\eta}_R(\boldsymbol{r}) = \sin\Theta(r)\hat{\boldsymbol{r}}\times\boldsymbol{\delta}_R \tag{4.2}$$

where $\boldsymbol{\delta}_R$ is a measure for the infinitesimal rotation. Similarly the translation defines

$$\boldsymbol{\eta}_T(\boldsymbol{r}) = \Theta'(r)\hat{\boldsymbol{r}}\hat{\boldsymbol{r}}\cdot\boldsymbol{\delta}_T + \frac{\sin\Theta(r)}{r}\left(\boldsymbol{\delta}_T - \hat{\boldsymbol{r}}\hat{\boldsymbol{r}}\cdot\boldsymbol{\delta}_T\right). \tag{4.3}$$

It is straightforward to verify that both $\boldsymbol{\eta}_R$ and $\boldsymbol{\eta}_T$ carry unit grand spin, *i.e.* these are dipoles in grand spin space. In accordance to the Skyrme model notation [7] we will refer to the channel which contains the rotational zero mode as magnetic dipole ($M1$) while the channel with the translational zero mode is called electric dipole ($E1$).

From the consideration of the zero modes we have obtained the quantum numbers of the fluctuations in the $M1$ and $E1$ channels. This allows us to make *ansätze*, which separate the radial and angular dependencies, for general fluctuations in these channels

$$\boldsymbol{\tau}\cdot\tilde{\boldsymbol{\eta}}_{M1}(\boldsymbol{r},\omega) = \boldsymbol{\tau}\cdot(\hat{\boldsymbol{r}}\times\boldsymbol{\zeta}(r,\omega)) = \frac{i}{2}\left[\boldsymbol{\tau}\cdot\boldsymbol{\zeta}(r,\omega), \boldsymbol{\tau}\cdot\hat{\boldsymbol{r}}\right] \tag{4.4}$$

and

$$\boldsymbol{\tau}\cdot\tilde{\boldsymbol{\eta}}_{E1}(\boldsymbol{r},\omega) = \boldsymbol{\tau}\cdot\boldsymbol{\zeta}_A(r,\omega) + \boldsymbol{\tau}\cdot\hat{\boldsymbol{r}}\boldsymbol{\tau}\cdot\boldsymbol{\zeta}_B(r,\omega)\boldsymbol{\tau}\cdot\hat{\boldsymbol{r}}. \tag{4.5}$$

Altogether these *ansätze* introduce nine radial functions. Although the parametrization (4.5) is not intuitively clear from (4.3) it is the most convenient one since the action of the grand spin zero object $\gamma_5\boldsymbol{\tau}\cdot\hat{\boldsymbol{r}}$ on the quark wave–functions $\tilde{\Psi}_\nu(\boldsymbol{r})$ is well-known [22] and does neither change grand spin nor parity quantum numbers. This knowledge is also the reason why we expressed $\tilde{\boldsymbol{\eta}}_{M1}$ in terms of a commutator. In order to compute the matrix elements of the *ansätze* (4.4) and (4.5) we thus only require the matrix elements of $\boldsymbol{\tau}$ times a radial function.

In the above notation the zero modes are parametrized by

$$\boldsymbol{\zeta}^{\text{z.m.}}(r) = \sin\Theta(r)\ \boldsymbol{\delta}_R \tag{4.6}$$

$$\boldsymbol{\zeta}_A^{\text{z.m.}}(r) = \frac{1}{2}\left(\Theta'(r) + \frac{\sin\Theta(r)}{r}\right)\boldsymbol{\delta}_T\ , \quad \boldsymbol{\zeta}_B^{\text{z.m.}}(r) = \frac{1}{2}\left(\Theta'(r) - \frac{\sin\Theta(r)}{r}\right)\boldsymbol{\delta}_T\ . \tag{4.7}$$

Now the main task is to substitute the *ansätze* (4.4) and (4.5) into the action functional. Although these calculations are straightforward they are quite tedious and we do not go into the details here. As a matter of fact the presentation of the associated formulae would approximately double the length of this paper. Let us rather display the generic form of the Bethe–Salpeter equations for radial functions defined above. As a matter of isospin invariance the action only depends on the combinations $\boldsymbol{\zeta}(r,\omega)\cdot\boldsymbol{\zeta}(r',-\omega)$ for the $M1$ channel on the one hand and $\boldsymbol{\zeta}_A(r,\omega)\cdot\boldsymbol{\zeta}_A(r',-\omega)$, $\boldsymbol{\zeta}_A(r,\omega)\cdot\boldsymbol{\zeta}_B(r',-\omega)$ as well as

$\boldsymbol{\zeta}_B(r,\omega)\cdot\boldsymbol{\zeta}_B(r',-\omega)$ for the $E1$ channel on the other hand. Thus the isospin invariance reduces the number of independent radial functions from nine to three. We label these by $\zeta(r,\omega)$, $\zeta_A(r,\omega)$ and $\zeta_B(r,\omega)$ and keep in mind that they are three–fold degenerate. This causes an overall factor 3 in eqn (3.23) when one considers the $M1$ and $E1$ channels. The Bethe–Salpeter equation for $\zeta(r,\omega)$ becomes an homogeneous integral equation in the radial coordinate

$$r^2\left\{\int dr'r'^2\Phi_2^{M1}(r,r',\omega^2)\zeta(r',\omega)+\Phi_1^{M1}(r)\zeta(r,\omega)\right\}=0 \tag{4.8}$$

while the Bethe–Salpeter equation for radial function in the electric channel couples $\zeta_A(r,\omega)$ and $\zeta_B(r,\omega)$

$$\begin{aligned} r^2\Bigg\{\int dr'r'^2\left[\Phi_2^{E1AA}(r,r',\omega^2)\zeta_A(r',\omega)+\Phi_2^{E1AB}(r,r',\omega^2)\zeta_B(r',\omega)\right]\\ +\Phi_1^{E1}(r)\left[\zeta_A(r,\omega)-\frac{1}{3}\zeta_B(r,\omega)\right]\Bigg\}=0 \end{aligned} \tag{4.9}$$

$$\begin{aligned} r^2\Bigg\{\int dr'r'^2\left[\Phi_2^{E1BB}(r,r',\omega^2)\zeta_B(r',\omega)+\Phi_2^{E1BA}(r,r',\omega^2)\zeta_A(r',\omega)\right]\\ +\Phi_1^{E1}(r)\left[\zeta_B(r,\omega)-\frac{1}{3}\zeta_A(r,\omega)\right]\Bigg\}=0 \end{aligned} \tag{4.10}$$

Upon explicit computation it can be shown that the non–diagonal elements of the Bethe–Salpeter kernel satisfy $\Phi_2^{E1AB}(r,r',\omega^2)=\Phi_2^{E1BA}(r',r,\omega^2)$ which, of course, reflects the Hermitian character of the Bethe–Salpeter kernel. As a further consequence the diagonal elements Φ_2^{M1} as well as Φ_2^{E1AA} and Φ_2^{E1BB} turn out to be symmetric.

The numerical treatment of equations like (4.8) is described at length in ref.[30]. Thus we will only explain the key steps. As the diagonalization (1.10) of the Dirac Hamiltonian (1.16) is performed utilizing a spherical box of radius D in order to discretize the momentum eigenstates this geometry transfers to the Bethe–Salpeter equation for the meson fluctuations. The radial coordinate is then discretized ($r_k=\triangle r(k-1),\ k=1,...,N$ and $r_N=D$ determines $\triangle r$) which transforms the integral equations into matrix equations. Then these matrix equations are extended to eigenvalue equations [25] by setting the RHS to $\lambda(\omega)\zeta(\boldsymbol{r},\omega)$. The eigenvalue $\lambda(\omega)$ then depends on the frequency ω. Finally ω is tuned to the eigen–frequency ω_i such that $\lambda(\omega_i)=0$. The associated eigenvector represents the eigen–wave–function in the descretized form. The bilocal parts of the kernels only involve matrix elements of h_1 (2.5). In these matrix elements upper and lower components of the Dirac spinors are coupled because h_1 is linear in γ_5. At $r=D$ the unitary transformation $\mathcal{T}$ (2.4) equals unity. Thus the integrands of the matrix elements of h_1 at $r=D$ are linear combinations of terms which are products of an upper and a lower component of the eigen–functions of h_0 at the boundary, $\Psi_\nu(|\boldsymbol{r}|=D)$. For reasons which will be explained below we impose boundary conditions on these eigen–spinors such that the upper components always vanish at $r=D$ [23]. It is then obvious that the bilocal parts of the kernels are zero as one of the arguments (r or r') lies on the boundary. On the other hand the local kernels have finite components at $r=D$. Thus the boundary conditions for the Dirac spinors imply boundary conditions for the meson fluctuations as well

$$\zeta(D,\omega)=\zeta_A(D,\omega)=\zeta_B(D,\omega)=0. \tag{4.11}$$

For finite D these conditions lead to discretized mesonic modes.

Since the algebraic expressions for the Bethe–Salpeter equations are by far too complicated to recognize the appearance of the zero modes we have to verify their existence numerically. In order to do so we diagonalize the discretized kernels for $\omega_i = 0$. Then we compare the wave–functions associated with the lowest eigenvalues with the radial functions given in eqns (4.6) and (4.7). The results are shown in figure 4.1 for the constituent quark mass $m = 400$MeV. The size of the spherical cavity is chosen to be $D = 6$fm, *i.e.* large compared to the typical extension of the soliton (1fm). For the rotational zero mode we find excellent agreement, while for the translational zero mode a small deviation can be observed in the vicinity of the origin. This, however, is due to the fact that the numerical computation of the derivative Θ' near $r = 0$ is burdened with some small errors. We should also mention that the lowest eigenvalue of the Bethe–Salpeter kernel at $\omega = 0$ is about three orders of magnitude smaller than the next to lowest one. *I.e.* the radial functions displayed in figure 4.1 are in fact solutions to the equations (4.8), (4.9) and (4.10). Thus we have also numerically established the existence of zero modes in the background field of the NJL soliton. Furthermore this verification provides an excellent check on our algebraical and numerical computations of the kernels which are quite involved.

Considering figure 4.1 the sizable slope of $\zeta_A^{\text{z.m.}}(r)$ indicates that the translational zero mode has non–negligible overlaps $\langle \tilde{\boldsymbol{\eta}}_{E1}^{\text{z.m.}}(\boldsymbol{r}) | \tilde{\boldsymbol{\eta}}^{(0)}(\boldsymbol{r}, \omega_j^{(0)}) \rangle$ with states of large $\omega_j^{(0)}$. Thus one might run into problems concerning the natural cut–off $\omega_{\text{thres}}^{(0)} = 2m$. We will concentrate on this when discussing the numerical results for the energy correction in the following section. First we have to define the metric for the $E1$ and $M1$ channels. In order to take account of the spherical symmetry we define the metric for the $M1$ channel in the discretized coordinate space (r_i) via

$$\mathcal{M}_{kl}^{M1}\omega_i) = (\triangle r)^2 \; r_k^2 r_l'^2 \frac{\partial}{\partial \omega^2} \Phi_2^{M1}(r_k, r_l', \omega)\Big|_{\omega=\omega_i} \tag{4.12}$$

while in the $E1$ channel

$$\mathcal{M}_{kl}^{E1}(\omega_i) = (\triangle r)^2 \; r_k^2 r_l'^2 \frac{\partial}{\partial \omega^2} \begin{pmatrix} \Phi_2^{E1AA}(r_k, r_l', \omega) & \Phi_2^{E1AB}(r_k, r_l', \omega) \\ \Phi_2^{E1BA}(r_k, r_l', \omega) & \Phi_2^{E1BB}(r_k, r_l', \omega) \end{pmatrix} \Bigg|_{\omega=\omega_i} \tag{4.13}$$

acts in the $2N$–component vector space spanned by $\begin{pmatrix} \zeta_{Ak}(\omega_i) \\ \zeta_{Bk}(\omega_i) \end{pmatrix}$. In the discretized coordinate space these metric tensors are symmetric matrices $\mathcal{M}_{kl}^{M1,E1}(\omega_i)$. In particular there exist transformations V's such that the $V^\dagger \mathcal{M} V$'s are diagonal. Then the roots (2.26) are defined via the eigenvalues* $\lambda_m^{M,E}(\omega_i)$ of $\mathcal{M}^{M1,E1}$

$$\left(\sqrt{\mathcal{M}}\right)_{kl}(\omega_i) = \left(V \cdot \text{diag}\left(\sqrt{\lambda_1(\omega_i)}, .., \sqrt{\lambda_N(\omega_i)}\right) \cdot V^\dagger\right)_{kl} \tag{4.14}$$

for the $M1$ and $E1$ channels separately. In the latter case the matrices are $2N \times 2N$ dimensional. According to (2.27) the metric is defined into the wave–functions which solve the Bethe–Salpeter equation

$$\phi_k^{M1}(\omega_i) \;\; = \;\; \triangle r \sum_l \left(\sqrt{\mathcal{M}}\right)_{kl}(\omega_i)\zeta_k(\omega_i) \tag{4.15}$$

*These eigenvalues should not be mixed up with the auxiliary eigenvalues, which were introduced to solve the Bethe–Salpeter equation.

$$\begin{pmatrix} \phi^{E1}_{Ak}(\omega_i) \\ \phi^{E1}_{Bk}(\omega_i) \end{pmatrix} = \triangle r \sum_l \begin{pmatrix} \left(\sqrt{\mathcal{M}}\right)^{AA}_{kl}(\omega_i) & \left(\sqrt{\mathcal{M}}\right)^{AB}_{kl}(\omega_i) \\ \left(\sqrt{\mathcal{M}}\right)^{BA}_{kl}(\omega_i) & \left(\sqrt{\mathcal{M}}\right)^{BB}_{kl}(\omega_i) \end{pmatrix} \cdot \begin{pmatrix} \zeta_{Al}(\omega_i) \\ \zeta_{Bl}(\omega_i) \end{pmatrix}. \quad (4.16)$$

These modified wave–functions are then subject to the trivial overall normalization

$$1 = \triangle r \sum_k \phi^{M1}_k(\omega_i)^2 \quad \text{and} \quad 1 = \triangle r \sum_k \left(\phi^{E1}_{Ak}(\omega_i)^2 + \phi^{E1}_{Bk}(\omega_i)^2\right). \quad (4.17)$$

Furthermore the overlaps are given by

$$\langle \tilde{\boldsymbol{\eta}}_{E1}(\boldsymbol{r},\omega_i) | \tilde{\boldsymbol{\eta}}^{(0)}(\boldsymbol{r},\omega^{(0)}_j)\rangle = \triangle r \sum_k \phi^{M1}_k(\omega_i)\phi^{(0)M1}_k(\omega^{(0)}_j) \quad (4.18)$$

$$\langle \tilde{\boldsymbol{\eta}}_{E1}(\boldsymbol{r},\omega_i) | \tilde{\boldsymbol{\eta}}^{(0)}(\boldsymbol{r},\omega^{(0)}_j)\rangle = \triangle r \sum_k \left(\phi^{E1}_{Ak}(\omega_i)\phi^{(0)E1}_{Ak}(\omega^{(0)}_j) + \phi^{E1}_{Bk}(\omega_i)\phi^{(0)E1}_{Bk}(\omega^{(0)}_j)\right). \quad (4.19)$$

Here $\phi^{(0)}$ represent the analogues of ϕ in the absence of the soliton.

Although we are now completely equipped to compute the energy correction $\triangle E$ we postpone this to the next section and rather add some comments on the normalization of the zero modes. One can easily show that substituting the rotational zero mode (4.2) into h_1 (2.5) corresponds to

$$h_1\left(\boldsymbol{\eta}_R\right) = \frac{i}{2}\left[\boldsymbol{\tau}\cdot\boldsymbol{\delta}_R, h_0\right] \quad (4.20)$$

with h_0 being the static Dirac Hamiltonian (1.16). Since, by definition, the zero mode has $\omega_i = 0$ one obtains for its normalization from eqn (2.23)

$$\begin{aligned} 1 &= \frac{N_C}{2}\eta^{\rm val}\sum_{\mu\neq{\rm val}}\frac{\langle {\rm val}|\boldsymbol{\tau}\cdot\boldsymbol{\delta}_R|\mu\rangle\langle\mu|\boldsymbol{\tau}\cdot\boldsymbol{\delta}_R|{\rm val}\rangle}{\epsilon_\mu - \epsilon_{\rm val}} \\ &\quad + \frac{N_C}{8}\sum_{\mu\nu}\langle\nu|\boldsymbol{\tau}\cdot\boldsymbol{\delta}_R|\mu\rangle\langle\mu|\boldsymbol{\tau}\cdot\boldsymbol{\delta}_R|\nu\rangle\left(\epsilon_\mu-\epsilon_\nu\right)^2\int_{1/\Lambda^2}^\infty ds\sqrt{\frac{s}{4\pi}}\int_0^1 dx \\ &\quad \times\left\{1 - sx(1-x)\left(\epsilon_\mu+\epsilon_\nu\right)^2\right\}\exp\left[-s\left((1-x)\epsilon_\mu^2 + x\epsilon_\mu^2\right)\right]. \end{aligned} \quad (4.21)$$

The Feynman parameter integral in this equation can be carried out resulting in

$$1 = \delta^a_R\delta^b_R\alpha^2_{ab} \quad (4.22)$$

where

$$\begin{aligned} \alpha^2_{ab} &= \frac{N_C}{2}\eta^{\rm val}\sum_{\mu\neq{\rm val}}\frac{\langle{\rm val}|\tau^a|\mu\rangle\langle\mu|\tau^b|{\rm val}\rangle}{\epsilon_\mu-\epsilon_{\rm val}} \\ &\quad + \frac{N_C}{4}\sum_{\mu\nu}\langle\nu|\tau^a|\mu\rangle\langle\mu|\tau^b|\nu\rangle\int_{1/\Lambda^2}^\infty\frac{ds}{\sqrt{4\pi s^3}}\left\{\frac{e^{-s\epsilon_\nu^2}-e^{-s\epsilon_\mu^2}}{\epsilon_\mu^2-\epsilon_\nu^2} - s\frac{\epsilon_\nu e^{-s\epsilon_\nu^2}+\epsilon_\mu e^{-s\epsilon_\mu^2}}{\epsilon_\nu+\epsilon_\mu}\right\} \end{aligned} \quad (4.23)$$

is just the moment of inertia for the chiral soliton [21] which actually turns out to be an isoscalar, $\alpha^2_{ab} = \alpha^2\delta^{ab}$. Thus we have shown that the rotational zero mode is normalized with respect to the moment of inertia. Analogously one can show that the translational zero mode is normalized with respect to the "pushing mass" tensor $E_{\rm push}\delta^{ab}$. This tensor is defined by replacing the isospin generators, τ^a in eqn (4.23) by the generators for the

infinitesimal translation, $i\partial_a$. In ref.[34] it has been demonstrated that the pushing mass is identical to the energy of the static soliton (1.14), *i.e.* $E_{\rm push} = E_{\rm cl}$. Thus the translational zero mode is indeed normalized with respect to the classical mass of the soliton. We may reverse these results and obtain a possibility to check our metric tensors $\mathcal{M}^{M1,E1}(\boldsymbol{r},\boldsymbol{r}',\omega = 0)$

$$\int d^3r \int d^3r' \boldsymbol{\zeta}_R^{\rm z.m}(\boldsymbol{r}) \cdot \mathcal{M}^{M1}(\boldsymbol{r},\boldsymbol{r}',\omega=0) \cdot \boldsymbol{\zeta}_R^{\rm z.m}(\boldsymbol{r}') \;=\; \alpha^2\ \boldsymbol{\delta}_R^2 \tag{4.24}$$

$$\int d^3r \int d^3r' \boldsymbol{\zeta}_T^{\rm z.m}(\boldsymbol{r}) \cdot \mathcal{M}^{E1}(\boldsymbol{r},\boldsymbol{r}',\omega=0) \cdot \boldsymbol{\zeta}_T^{\rm z.m}(\boldsymbol{r}') \;=\; E_{\rm cl}\ \boldsymbol{\delta}_T^2 \tag{4.25}$$

where the matrix structure of $\mathcal{M}^{E1}$ is not explicitly shown. Eqns (4.24) and (4.25) provide a possibility to check our calculations in the sense that we first compute the metric tensors for $\omega = 0$ and evaluate the integrals on the LHS by substituting eqns (4.6) and (4.7). These results are then compared with the direct evaluations of $E_{\rm cl}$ (1.14) and α^2 (4.23). Numerically we observe deviations as small of 0.1% when box sizes of the order $D = 6$fm are used and the explicit form in terms of the chiral angle is substituted in the integrals. When the solutions to the Bethe–Salpeter equations at $\omega = 0$ are employed to evaluate the integrals the error is somewhat larger because these solutions do not exactly match the explicit forms at very large radial distances. In any event this error has to be considered small and thus provides an excellent verification of the correctness of our algebraical as well as numerical manipulations which are rather involved.

The appearance of the moment of inertia also determined the above mentioned choice for the boundary conditions on the Dirac spinors Ψ_ν. For other boundary conditions, *e.g.* those suggested by Kahana and Ripka [22], the moment of inertia is plagued by isospin violations of the order $1/D$ [23].

5. Numerical Results

In the previous section we have already presented one of our main numerical results: We have verified the existence of rotational and translational zero modes. Before concentrating on the results for the energy subtraction $\triangle E$ we wish to add a few remarks on the solutions in the $M1$ and $E1$ channels when no soliton is present, *i.e.* $\Theta(r) \equiv 0$. These solutions are important for the overlaps $\langle \boldsymbol{\eta}^{\rm z.m.} | \boldsymbol{\eta}^{(0)} \rangle$. The $M1$ channel comes with unit orbital angular momentum, $l = 1$; *i.e.* a P–wave. Thus the corresponding solutions to the Klein Gordon equation which satisfy the boundary conditions (4.11) read

$$\zeta_{\rm free}(r,\omega_i^{(0)}) \propto j_1(q_i^1 r) \tag{5.1}$$

where the q_i^l make the $l^{\rm th}$ spherical Bessel function vanish at the boundary, $j_l(q_i^l D) = 0$. Furthermore $\omega_i^{(0)} = \sqrt{m_\pi^2 + (q_i^1)^2}$. In the $E1$ channel the situation is somewhat more involved since S–wave solutions

$$\zeta_{A,\rm free}(r,\omega_i^{(0)}) \propto j_0(q_i^0 r) \text{ and } \zeta_{B,\rm free}(r,\omega_i^{(0)}) = 0 \quad \text{with} \quad \omega_i^{(0)} = \sqrt{m_\pi^2 + (q_i^0)^2} \tag{5.2}$$

as well as D–wave solutions

$$\zeta_{A,\rm free}(r,\omega_i^{(0)}) \propto j_2(q_i^2 r) \text{ and } \zeta_{B,\rm free}(r,\omega_i^{(0)}) \propto 3j_2(q_i^2 r) \quad \text{with} \quad \omega_i^{(0)} = \sqrt{m_\pi^2 + (q_i^2)^2} \tag{5.3}$$

exist. We have then computed the solutions to the Bethe–Salpeter equation (2.16) in the absence of the soliton and compared these results with the above suggested solutions to

the Klein–Gordon equation. In figure 5.1 we display a typical solution in the $M1$ channel. Here we have chosen $m_\pi = 0$. From eqn. (2.16) we obtain for this solution the eigen–frequency $\omega^{(0)} = 360.1$MeV which reasonably well compares with 363.5MeV as indicated by the root $q_3^1 D$ of the spherical Bessel function. Except for a small vicinity of $r = D$ the radial behavior of our solution to eqn (2.16) matches that of the associated spherical Bessel function $j_1(q_3^1 r)$. In figure 5.2 the same comparison is performed for the S– and D–wave solutions in the $E1$ channel. Again the eigen–frequencies which are suggested by the solutions of the Klein–Gordon equation are reproduced at the order of 1% and the radial dependencies of the solutions to eqn (2.16) reasonably well agree with the corresponding Bessel functions. This is especially the case for $r \leq D/2$. Since we are interested in the overlap with the zero modes, which are well localized (*cf.* figure 4.1) the deviation from the Bessel functions at $r \approx D$ is negligible because this region is not relevant for the overlap. Thus we may approximate the solutions to eqn (2.16) in the absence of the soliton by the spherical Bessel functions as suggested in eqns (5.1), (5.2) and (5.3). This represents a major simplification because solving eqn (2.16) numerically is very time consuming*. This is in particular the case for the $E1$ channel since the solutions corresponding to the roots q_i^0 and q_i^2 lie quite close and are difficult to disentangle numerically.

We thus employ the following procedure to evaluate the matrix elements $\langle \boldsymbol{\eta}^{\text{z.m.}} | \boldsymbol{\eta}^{(0)} \rangle$: We firstly reproduce the zero mode wave–function from the Bethe–Salpeter equation in the presence of the soliton and compute the associated metric tensor. This then provides the modified wave–functions $\phi^{\text{z.m.}}(r)$ in both the $M1$ and $E1$ channels according to eqns (4.15) and (4.16). Next we compute the metric tensors in the absence of the soliton for the frequencies $\omega_i^{(0)}$ determined by the roots of the Bessel functions. Substituting the approximations (5.1), (5.2) and (5.3) into eqns (4.15) and (4.16) in turn leads to the modified wave–functions $\phi^{(0)}(r)$. After normalizing these wave–functions according to eqn (4.17) we are finally enabled to compute the relevant matrix elements as prescribed in eqns (4.18) and (4.19). In the course of these calculations we encounter one further problem. Due to numerical errors some eigenvalues of the metric tensors turn out to be negative yielding eqn (4.14) ill–defined. As a matter of fact the absolute values of these negative eigenvalues turn out to be about three orders of magnitude smaller than the relevant positive ones. In any event we do not expect a numerical accuracy better than about 1%. We therefore ignore these negative eigenvalues. This in some sense defines a truncated norm. The validity of this treatment can be judged by first normalizing $\boldsymbol{\eta}$ subject to $\int d^3r \int d^3r' \boldsymbol{\eta}(\boldsymbol{r}) \cdot \mathcal{M}(\boldsymbol{r}, \boldsymbol{r}') \cdot \boldsymbol{\eta}(\boldsymbol{r}') = 1$. Then the modified wave–functions $\boldsymbol{\phi}$ are computed with the truncated norm. Numerically we then find the normalization of ϕ to deviate from unity by less than 0.01%. This, of course, justifies the above truncation of the norm which turned out to be necessary as a consequence of the numerical inaccuracy.

We have now completed the presentation of the methods and treatments which serve as input to compute the energy correction $\triangle E$. Needless to mention that we also substitute the roots of the Bessel functions for $\omega_j^{(0)}$ in eqn (3.23). We have already mentioned that, a as consequence of the non–confining NJL model, real solutions only exist for $\omega_j^{(0)} \leq 2m$. Due to the treatment in a finite box of radius D the lowest quark energy is $\sqrt{m^2 + (\pi/D)^2}$

*The computation of the kernels $\Phi_{1,2}^{E1}$ for a given frequency ω takes about 20h-cpu on a HP9000/710 workstation. In this context it should be remarked that the auxiliary eigenvalues of the Bethe–Salpeter kernel for $\Theta \equiv 0$ depend on ω rather strongly. It turns out that ω has to be adjusted with an accuracy better than 0.1% in order to solve the Bethe–Salpeter equation.

Table 5.1: The quantum corrections to the soliton mass due to the rotational zero mode. The size of the spherical cavity is $D = 6$fm.

	$m_\pi = 0$			$m_\pi = 135$MeV		
m(MeV)	400	500	600	400	500	600
$\mathcal{S}$	0.88	0.94	0.95	0.83	0.89	0.91
$\triangle E$(MeV)	-201	-274	-290	-244	-297	-323

which increases the threshold energy to $\omega^{\rm th} = 2\sqrt{m^2 + (\pi/D)^2}$ in the $M1$ channel while in the $E1$ channel[†] $\omega^{\rm th} = \sqrt{m^2 + (\pi/D)^2} + \sqrt{m^2 + (q_1^1)^2}$. We therefore truncate the sum (3.23) accordingly. In order to judge this truncation we define the sum of overlaps for the zero modes

$$\mathcal{S} = \sum_{\omega_j^{(0)} \leq \omega^{\rm th}} \left| \langle \tilde{\boldsymbol{\eta}}^{\rm z.m.}(\boldsymbol{r}) | \tilde{\boldsymbol{\eta}}^{(0)}(\boldsymbol{r}, \omega_j^{(0)}) \rangle \right|^2 \tag{5.4}$$

which should approach unity if the model were insensible to the truncation. Note that the number of meson modes which lie below $\omega^{\rm th}$ decreases as m_π increases.

In table 5.1 the results for the rotational zero mode are presented. We see that the sum of overlaps $\mathcal{S}$ is about 0.9 for all sets of parameter used. This number, of course, increases with the constituent quark mass m because the threshold grows proportionally. Furthermore $\mathcal{S}$ is sufficiently close to unity in order to conclude that the energy subtraction $\triangle E \approx -(250 - 300)$MeV is reliable. Actually this is about 100MeV smaller than the corresponding value in the Skyrme model [14]. We also observe that the mass correction due to the rotational zero mode is about (30-40)MeV lower in the chiral limit than for the physical value of the pion mass, $m_\pi = 135$MeV.

Table 5.2 contains the results for the translational zero mode. We see that the sum of overlaps is significantly smaller than for the rotational zero mode (table 5.1). Here it hardly reaches 0.5. This is due to the fact that the slope of the profile function corresponding to the translational zero mode is enhanced compared to that of the rotational zero mode. Thus a sizable number of Fourier components with non–vanishing overlap lie beyond the quark–antiquark threshold. Hence we have to interpret the resulting $\triangle E \approx -(100 - 200)$MeV as a lower bound for the energy subtraction originating from the translational zero mode. Nevertheless we can extract some qualitative statements from the results listed in table 5.2. First of all we observe that the D–wave contributions are dominating. This result is also found in the Skyrme model [14]. Furthermore we see that the value of the pion mass has only little influence on the S–wave contribution while the absolute value of the D–wave contribution decreases with increasing pion mass. This is in contrast to the rotational zero mode. Thus the net effect of varying the pion mass is somewhat mitigated.

Next we wish to estimate the contributions of the scattering states, $\omega_i \geq m_\pi$, to the energy correction $\triangle E$ as described by eqn (3.23). In order to do so we first have to construct the corresponding solutions to the Bethe–Salpeter equation (2.16). In table 5.3 the frequencies of the lowest solutions are compared to their analogues in the absence of the soliton. In the $E1$ channel we distinguish between solutions which are dominantly S–

[†]Note that in the $E1$ channel h_1 has vanishing matrix elements in the grand spin zero subsystem of the quark modes.

Table 5.2: The quantum corrections to the soliton mass due to the translational zero mode. The contributions stemming from the $S(l=0)$– and $D(l=2)$–waves are disentangled. The size of the spherical cavity is $D = 6$fm.

	$m_\pi = 0$			$m_\pi = 135$MeV		
m(MeV)	400	500	600	400	500	600
$\mathcal{S}$	0.41	0.41	0.61	0.28	0.37	0.46
$\triangle E_{l=0}$(MeV)	-18	-22	-28	-12	-22	-28
$\triangle E_{l=2}$(MeV)	-127	-140	-207	-82	-128	-187
$\triangle E$(MeV)	-145	-162	-235	-94	-150	-215

Table 5.3: The contribution of the first scattering states to the quantum corrections of the soliton mass in the channel of the rotational ($M1$) and translational ($E1$) zero modes. The scattering state under consideration is labeled η. The entry "max(..)" represents the contribution to $\mathcal{S}$ by the dominant term. The constituent quark and the pion masses are 600MeV and 135MeV, respectively. The size of the spherical cavity is $D = 6$fm.

	$M1$	$E1$	
	$l=1$	$l=0$	$l=2$
$\omega^{(0)}$(MeV)	202	171	235
ω(MeV)	210	176	240
$\max\left(\langle\boldsymbol{\eta}_i^{(0)}\vert\boldsymbol{\eta}\rangle^2\right)$	0.96	1.00	0.99
$\mathcal{S}$	0.99	1.00	1.00
$\triangle E$(MeV)	-1.9	-0.6	-0.5

or D–waves. We establish that the scattering states always lie slightly above the associated states for $\Theta = 0$. We furthermore observe from table 5.3 that the sum over the overlaps $\mathcal{S}$ is strongly dominated by only one term. As a matter of fact it is always the one which happens to have the same number of knots in the radial part of the wave–function associated with scattering state under consideration. This dominance causes $\mathcal{S}$ to very closely approach unity. Thus we conclude that the contribution of the low–lying scattering states to $\triangle E$ of the order of only a few MeV is very reliable. We have found the same result for the second scattering state in the $M1$ channel. For the $E1$ channel the extraction of higher scattering states is somewhat troublesome because the states which are dominantly S– or D–waves are almost degenerate. Nevertheless the results found so far for the scattering states suggest that their contribution to $\triangle E$ is almost negligible. The fact that these contributions turn out to be negative is a consequence of the expansion (3.21) when the "perturbation" V is attractive [35]. These results qualitatively agrees with those obtained in the Skyrme model [14].

We are finally enabled to present our predictions for the masses of baryons in the NJL soliton approach. For the projection onto good quantum numbers of spin and isospin we employ the well–established semi–classical cranking approach [3]. This yields the mass formula for a baryon of spin J

$$M = E_{\rm cl} + \triangle E + \frac{J(J+1)}{2\alpha^2}. \tag{5.5}$$

Table 5.4: The predictions for the masses of the nucleon (N) and Δ–resonance. The empirical data are 939MeV and 1232MeV, respectively.

	$m_\pi = 0$			$m_\pi = 135$MeV		
m(MeV)	400	500	600	400	500	600
$E_{\rm cl}$(MeV)	1212	1193	1166	1250	1221	1193
$\triangle E$(MeV)	-346	-436	-525	-338	-448	-538
α^2(1/GeV)	6.26	4.73	3.87	5.80	4.17	3.43
M_N(MeV)	926	836	738	976	863	764
M_Δ(MeV)	1166	1153	1126	1236	1223	1201

According to the above discussions $\triangle E$ is understood as the sum of the zero mode contributions listed in tables 5.1 and 5.2. In eqn (5.5) α^2 refers to the moment of inertia (4.23,4.24) [21]. The individual pieces in eqn (5.5) are of the orders $\mathcal{O}(N_C)$, $\mathcal{O}(1)$ and $\mathcal{O}(1/N_C)$, respectively. Here we have ignored the quantum corrections at order $\mathcal{O}(1/N_C)$. These have been estimated in the Skyrme model to be less than 100MeV [14]. Hence their contribution seems to be less than the uncertainties in our estimates for $\triangle E$.

We indeed find that the numerical results roughly follow this $1/N_C$ counting pattern. Unfortunately the results shown in table 5.4 suggest that the overall prediction for the baryon masses in the NJL soliton model underestimates the empirical value for the nucleon mass (939MeV). Only for the constituent quark mass $m \approx 400$MeV a good description is obtained. In that case, however, $\mathcal{S}$ is as small as 0.4 in the $E1$ channel (*cf.* table 5.2). Then, of course, the question of reliability cannot be answered unambiguously. Although one may assume the point of that this is a shortcoming of the NJL model in general rather than only for the meson fluctuations. Hence one would have to consider the results listed in tables 5.1 and 5.2 seriously and conclude that the masses of the nucleon and Δ–resonance are reasonably well reproduced for $m \approx 400$MeV. As m is further increased the classical soliton energy $E_{\rm cl}$ as well as the quantum corrections decrease; thereby underestimating the nucleon mass. Simultaneously the $1/N_C$ counting pattern breaks down since also the moment of inertia, α^2, decreases leading to a Δ–nucleon mass splitting of the order of $\triangle E$. These two quantities are, however, supposed to differ by one order in N_C. In turn this renders the prediction for the mass of the Δ–resonance almost independent of the parameters and in reasonable agreement with experimental value of 1232MeV when the physical value of the pion mass is adopted.

6. Conclusions

In the present paper we have studied the quantum corrections, $\triangle E$, to the classical mass, $E_{\rm cl}$, of the chiral soliton in the NJL model. In a first step we have investigated the formal structure of the Bethe–Salpeter equation for pionic fluctuations in the soliton background. As the soliton is static and the eigen–modes of this equation appear in pairs $\pm\omega_i$ we were able to demonstrate that the energy operator in the Fock space of the meson fluctuations is identical to that of a harmonic oscillator; although the time derivative operator appears at all (even) orders in the coordinate space representation of the Bethe–Salpeter equation. This result has allowed us to adopt the expression for the quantum correction which was previously obtained in the Skyrme model [14]. According to our examinations this expression is applicable to all static soliton models in $3+1$ dimensions as

long as the eigen–modes occur in pairs. However, here the overlap matrix element between solutions of the Bethe–Salpeter equation with and without the soliton present, has turned out to be more involved than in the Skyrme model in particular because the solutions in the absence of the soliton do not exactly obey the Klein–Gordon equation. Furthermore the sum over the free eigen–modes had to be truncated since these modes are unstable against the decay into a quark–antiquark pair once the corresponding eigen–frequency has exceeded the threshold, $2m$.

Two types of eigen–modes exist in the presence of the soliton: The bound zero modes and the scattering states. We have made plausible that the latter type only contributes very little to $\triangle E$. Hence the scattering modes have been discarded and $\triangle E$ has completely been approximated by the zero mode contribution. This procedure is also justified by the similar calculations in the Skyrme model [14].

Before actually computing the quantum corrections we have, for the first time, verified the existence of rotational and translation zero modes in the background of the NJL soliton by explicit construction. For the rotational zero mode the truncation caused by the non–confining nature of the NJL model of the mode sum does not represent a serious problem because the sum of overlaps approximates unity fairly well. This in turn leads to a reliable estimate for the quantum correction due to the rotational zero mode of about -250MeV. In the case of the translational zero mode the situation is somewhat worse because the overlaps sum up to only about 0.5. In this sense one has to regard $\triangle E \approx -150$MeV only as a bound.

One might, however, adopt a different point of view and consider the above quoted data as the actual results. In any event the NJL model is not well defined for frequencies above the quark–antiquark threshold. All other quantities (*e.g.* the classical mass $E_{\rm cl}$) might undergo significant changes as well once the model is improved to avoid this problem. In this interpretation we have observed that the NJL model predicts the masses of the nucleon and the Δ resonance fairly well for a constituent quark mass $m \approx 400$MeV. Even the $1/N_C$ counting scheme $E_{\rm cl} \sim N_C \triangle E \sim N_C^2 (M_\Delta - M_N)$ seems to operate then. Upon increasing the constituent quark mass this is no longer the case and the estimate for the nucleon mass turns out to be somewhat too small while the prediction for M_Δ remains almost unaltered. The smallness of the absolute value for the nucleon mass appears to be connected to the fact that $E_{\rm cl}$ decreases as the constituent quark mass increases. This seems to be special to the NJL model without the isoscalar–vector ω–meson included. Recently it has been demonstrated that the proper incorporation of this field indeed yields a classical energy which increases with m [36]. Thus one might suspect that the associated extension of the NJL soliton model leads to an even more reasonable description of the nucleon mass for larger constituent quark masses. This would in a sense be more reliable because the sum of overlap matrix elements would come closer to unity.

As a side–product we have been able to define a metric for the overlaps of the meson states with and without the soliton present. As has previously been pointed out in the context of the Skyrme model [31] this metric plays an important role for the computation of the momentum dependent pion–nucleon form factor $g_{\pi NN}(q^2)$. In order to compute $g_{\pi NN}(q^2)$ one naïely would Fourier–transform $\sin\Theta(r)$. Commonly in soliton models this procedure underestimates the cut-off $\Lambda_{\pi NN} \approx 1.6$GeV, which is defined via

$$\frac{g_{\pi NN}(q^2<0)}{g_{\pi NN}(m_\pi^2)} = \frac{\Lambda_{\pi NN}^2 - m_\pi^2}{\Lambda_{\pi NN}^2 - q^2} \tag{6.1}$$

by a factor two or even more [37]. This may be improved by the proper incorporation of

the metric tensor because the Fourier–transformation of $\sin\Theta(r)$ basically represents the projection of the rotational zero mode onto free pion states. Investigations in this direction in the context of the NJL model are subject to future studies.

Acknowledgement

The authors gratefully acknowledge stimulating discussions with G. Holzwarth on the quantum corrections in soliton models.

References

[1] G. 't Hooft, Nucl. Phys. **B72** (1974) 461.

[2] E. Witten, Nucl. Phys. **B160** (1979) 57.

[3] G. S. Adkins, C. R. Nappi and E. Witten, Nucl. Phys. **B228** (1983) 552.

[4] T. H. R. Skyrme, Proc. R. Soc. **A260** (1661) 127.

[5] G. Holzwarth and B. Schwesinger, Rep. Prog. Phys. **49** (1986) 825;
I. Zahed and G. E. Brown, Phys. Rep. **142** (1986) 1.

[6] E. Braaten, S.–M. Tse and C. Willcox, Phys. Rev. Lett. **56** (1986) 2008.

[7] H. Walliser and G. Eckart, Nucl. Phys. **A429** (1984) 514;
G. Eckart, A. Hayashi and G. Holzwarth, Nucl. Phys. **A448** (1986) 732;
M. P. Mattis, M. Karliner, Phys. Rev. **D31** (1985) 2833.

[8] B. Schwesinger, H. Weigel, G. Holzwarth and A. Hayashi, Phys. Rep. **173** (1989) 173.

[9] "Baryons as Skyrme Solitons", G. Holzwarth (Ed.), World Scientific Publ. Comp., Singapore 1993.

[10] Ulf-G. Meißner, Phys. Rep. **161** (1988) 213;
P. Jain, R. Johnson, Ulf-G. Meißner, N. W. Park and J. Schechter, Phys. Rev. **D37** (1988) 3252;
Ulf-G. Meißner, N. Kaiser, H. Weigel and J. Schechter, Phys. Rev. **D39** (1989) 1956.

[11] S. Brodsky, J. Ellis and M. Karliner, *Phys. Lett.* **B206**, 309 (1988);
J. Ellis and M. Karliner, *Phys. Lett.* **B313**, 131 (1993);
J. Schechter, A. Subbaraman and H. Weigel, *Phys. Rev.* **D48**, 339 (1993).

[12] B. Moussallam and D. Kalafatis, Phys. Lett. **B272** (1991) 196.

[13] G. Holzwarth, Phys. Lett. **B291** (1992) 196.

[14] G. Holzwarth, Nucl. Phys. **A572** (1994) 69.

[15] D. Ebert and H. Reinhardt, Nucl. Phys. **B271** (1986) 188.

[16] Y. Nambu and G. Jona-Lasinio, Phys. Rev. **122** (1961) 345; **124** (1961) 246.

[17] For a recent review see *e.g.* T. Hatsuda and T. Kunihiro, "QCD Phenomenology based on a Chiral Effective Lagrangian". Phys. Rep., to be published.

[18] H. Reinhardt and R. Wünsch, Phys. Lett. **B215** (1988) 577; Phys. Lett. **B230** (1989) 93;
T. Meissner, F. Grümmer and K. Goeke, Phys. Lett. **B227** (1989) 296;
R. Alkofer, Phys. Lett. **B236** (1990) 310.

[19] H. Reinhardt, Phys. Lett. **B244** (1990) 316.

[20] J. Schwinger, Phys. Rev. **82** (1951) 664.

[21] H. Reinhardt, Nucl. Phys. **A503** (1989) 825.

[22] S. Kahana and G. Ripka, Nucl. Phys. **A429** (1984) 462.

[23] H. Weigel, R. Alkofer and H. Reinhardt, Nucl. Phys. **B387** (1992) 638;
A. Blotz, D. Diakonov, K. Goeke, N. W. Park, V. Petrov, and P. V. Pobylitsa, Nucl. Phys. **A555** (1993) 765.

[24] R. Alkofer, H. Reinhardt, J. Schlienz and H. Weigel, "Topologically non–trivial chiral transformations: The chiral invariant elimination of the axial vector meson field", hep-ph/9406420.

[25] H. Weigel, H. Reinhardt and R. Alkofer, Phys. Lett. **B313** (1993) 377.

[26] H. Weigel, R. Alkofer and H. Reinhardt, "Hyperons in the bound state approach to the Nambu–Jona–Lasinio chiral soliton", hep-ph/9310309, Nucl. Phys. **A576**, to be published.

[27] H. Weigel, R. Alkofer and H. Reinhardt, Phys. Rev. **D49**, 5958 (1994).

[28] H. Reinhardt and B. V. Dang, Nucl. Phys. **A500** (1989) 563.

[29] R. Alkofer and H. Weigel, "Self–consistent solution to a fermion determinant with space dependent fields", Computer Physics Communications, to be published.

[30] H. Weigel and R. Alkofer, "The Bethe–Salpeter equation for mesons as quark – anti-quark bound states in a soliton background", Computer Physics Communications, to be published.

[31] G. Holzwarth, G. Pari and B. K. Jennings, Nucl. Phys. **A515** (1990) 665.

[32] K. Cahill, A. Comtet and R. J. Glauber, Phys. Lett. **64B** (1976) 283.

[33] "Solitons and Instantons", R. Rajaraman, North–Holland Publishing Company, Amsterdam (1982).

[34] P. V. Pobylitsa, E. Ruiz Arriola, T. Meissner, F. Grümmer, K. Goeke and W. Broniowski, J. Phys. **G18** (1992) 1455.

[35] G. Holzwarth, private communication.

[36] H. Weigel, U. Zückert, R. Alkofer and H. Reinhardt, "On the analytic properties of chiral solitons in the presence of the ω–meson" hep-ph/9407304.

[37] T. D. Cohen, Phys. Rev. **D34** (1986) 2187;
N. Kaiser, Ulf-G. Meißner and W. Weise, Phys. Lett. **B198** (1987) 319;
P. Alberto, E. Ruiz Arriola, M. Fiolhais, F. Grümmer, J. N. Urbano and K. Goeke Phys. Lett. **B208** (1988) 75.

Figure captions

Figure 4.1

Comparison of the numerical solution of the Bethe–Salpeter equations (4.8,4.9,4.10) with the analytic form for the zero modes as given in eqns (4.6) and (4.7). The lattice points are indicated.

Figure 5.1

Comparison of the numerical solution of the Bethe–Salpeter equations (2.16) for $\Theta = 0$ with the corresponding spherical Bessel function in the $M1$ channel. Both curves refer to the wave–function of the second excited state. The normalization of the radial functions is arbitrarily chosen. The lattice points are indicated.

Figure 5.2

Comparison of the numerical solution of the Bethe–Salpeter equations (2.16) for $\Theta = 0$ with the corresponding spherical Bessel function in the $E1$ channel. Left: The S–wave solution with $\zeta_B(r) \equiv 0$. The normalization of the radial functions is arbitrarily chosen. The corresponding solution of the Klein–Gordon eqn has $\omega^{(0)} = 314.2$MeV. Right: The D–wave solution. Here the linear combination $\zeta_A(r) - \zeta_B(r)/3$ vanishes. The Klein–Gordon eqn yields the eigen–frequency 303.2MeV.

This figure "fig1-1.png" is available in "png" format from:

http://arXiv.org/ps/hep-ph/9408343v1

This figure "fig1-2.png" is available in "png" format from:

http://arXiv.org/ps/hep-ph/9408343v1

This figure "fig1-3.png" is available in "png" format from:

http://arXiv.org/ps/hep-ph/9408343v1

Figure 5.2

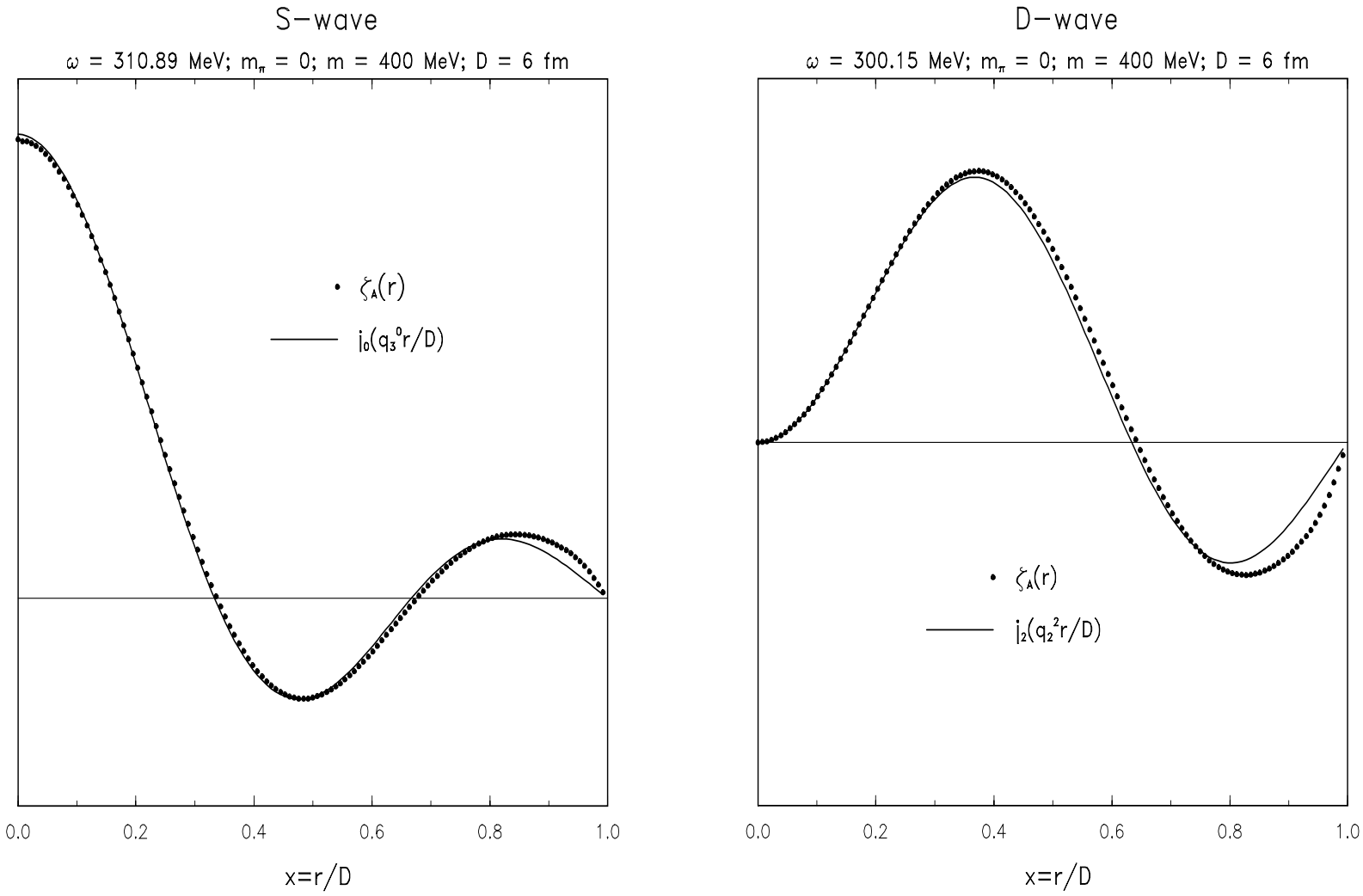
S−wave
ω = 310.89 MeV; m_π = 0; m = 400 MeV; D = 6 fm
• ζ_A(r)
j_0(q_3^0 r/D)
0.0
0.2
0.4
0.6
0.8
1.0
x=r/D
D−wave
ω = 300.15 MeV; m_π = 0; m = 400 MeV; D = 6 fm
• ζ_A(r)
j_2(q_2^2 r/D)
0.0
0.2
0.4
0.6
0.8
1.0
x=r/D

Figure 5.1

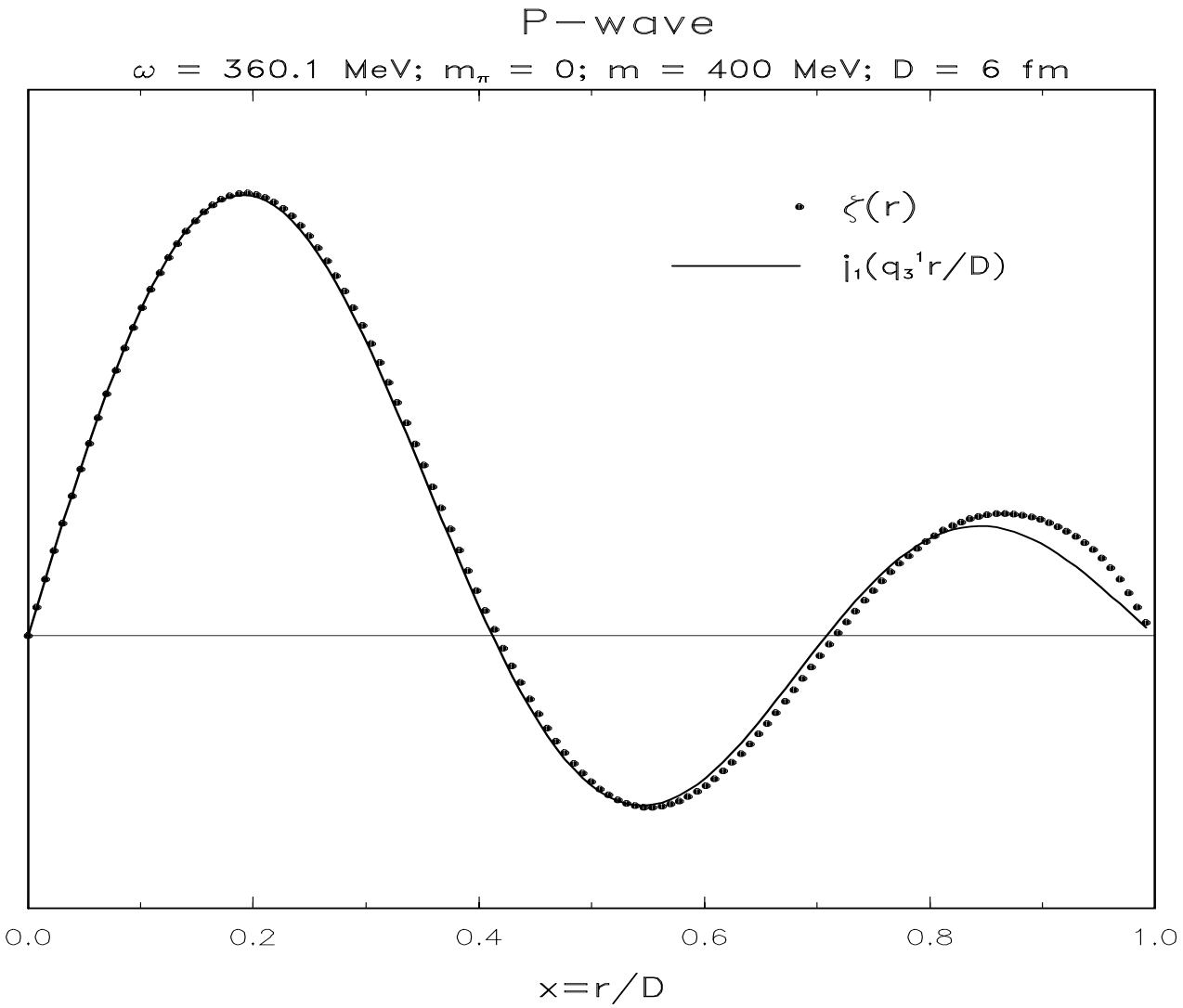
P—wave
ω = 360.1 MeV; m_π = 0; m = 400 MeV; D = 6 fm
ζ(r)
j₁(q₃¹r/D)
0.0
0.2
0.4
0.6
0.8
1.0
x=r/D

Figure 4.1

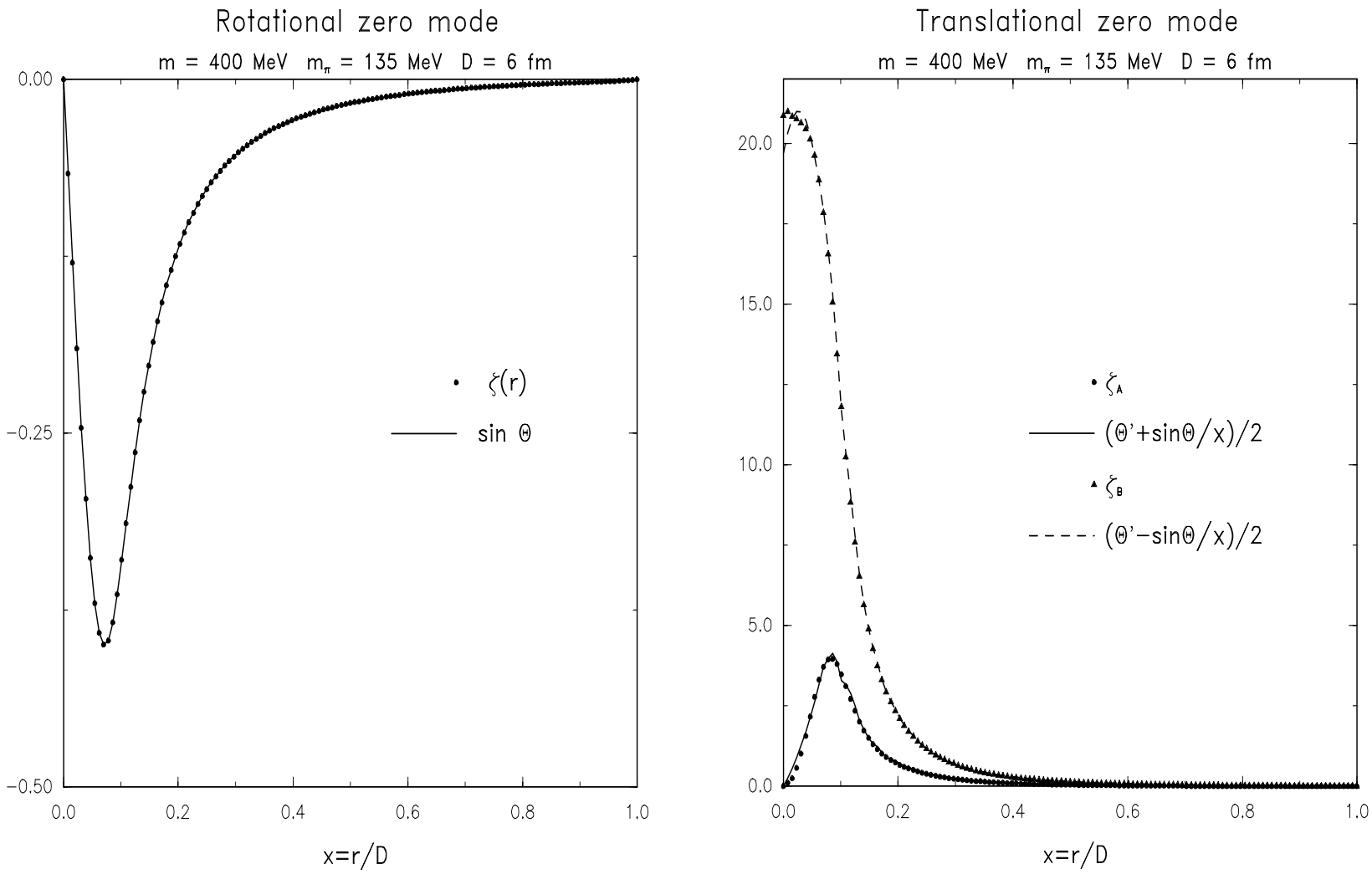
Rotational zero mode
m = 400 MeV m$_\pi$ = 135 MeV D = 6 fm
0.00
−0.25
−0.50
0.0
0.2
0.4
0.6
0.8
1.0
x=r/D
ζ(r)
sin Θ
Translational zero mode
m = 400 MeV m$_\pi$ = 135 MeV D = 6 fm
20.0
15.0
10.0
5.0
0.0
0.0
0.2
0.4
0.6
0.8
1.0
x=r/D
ζ$_A$
(Θ'+sinΘ/x)/2
ζ$_B$
(Θ'−sinΘ/x)/2